C.P. No. 722

C.P. No. 722

MINISTRY OF AVIATION

AERONAUTICAL RESEARCH COUNCIL

CURRENT PAPERS

A Study on the Running Times in Shock Tubes

By

J.A.D. Ackroyd

Department of Aeronautical Engineering,
Queen Mary College

LONDON: HER MAJESTY'S STATIONERY OFFICE

1964

TEN SHILLINGS NET

C.P. No.722

A Study on the Running Times in Shock Tubes

- By -
J. A. D. Ackroyd,
Department of Aeronautical Engineering,
Queen Mary College

July, 1963

SUMMARY

A review is presented of previous theoretical work for the prediction of shock-tube running times. A new analysis is then introduced which attempts to avoid most of the restrictive assumptions of the previous analyses which are shown to lead to large errors particularly at low shock Mach numbers. The new analysis and the previous analyses are compared with one another and with the existing experimental data. Further experimental work is presented and compared in conjunction with the existing experimental data with the results of the previous analyses and the present analysis.

It is shown that there is a distinct improvement in the prediction of shock-tube running times when the present analysis is used, particularly at low initial channel pressures and low shock Mach numbers.

Suggestions are finally included for the extension of the experimental work, and for the modification of the present analysis to include such phenomena as real-gas effects, shock-wave attenuation, and contact-region mixing.

CONTENTS/

Replaces A.R.C. 24 942.

CONTENTS

---

1. Introduction

It is a matter of experience that the running time in a shock tube can be much less than the predictions of simple theory based on an ideal (i.e. inviscid, non-conducting) perfect gas model. The running time at some distance from the diaphragm we define to be the time between the arrival of the primary shock wave and that of the contact surface, or region, at that distance from the diaphragm. In this statement we infer nothing about the variation of the usual gas parameters during this time.

We shall later refer to gas models which are non-ideal, and by this we mean gas models which allow for viscosity and heat conduction only.

The/

The term 'real gas' is applied only to gas models which allow for the changes of molecular structure brought about by dissociation, ionization, etc. Thus a perfect gas is understood to refer to a gas model in which the latter 'real-gas effects' are not considered.

Various attempts have been made to account for the variation between simple theory and experiment. Henshall[1] has estimated the corrections needed for a real-gas model, and has shown, for example, that for a shock Mach number of 20 in air, the running time might be expected to be about 50% of the predictions of simple theory. However, for a shock Mach number of 6 in air, the discrepancy between simple theory and Henshall's real-gas calculations is approximately 15%, whereas experimenters have reported running times of the order of 70% less than the predictions of simple theory for shock Mach numbers much lower than 6 for conditions where real-gas effects are known to be negligibly small. Hence it appears that for low shock Mach numbers at least, the solution to the running-time problem lies elsewhere.

More recently the attempts to predict shock-tube running times have been directed to explaining the difference between experiment and ideal-gas theory by appeal to boundary-layer theory. There are indeed many strong indications that the explanation lies in the non-ideal properties of the gases. Duff[2], for example, has shown experimentally that the running time can depend strongly on the initial channel pressure, and in fact the experimental evidence shows a nearly linear relationship between the latter two quantities for channel pressures less than 5 mm Hg with a shock Mach number of 1·6 in argon. Duff then argues on dimensional grounds that for a constant shock Mach number, and assuming that a laminar boundary layer develops behind the shock, one may expect the ratio of running time to initial channel pressure to be constant. This, then, leads to the linear relationship between running time and initial channel pressure suggested by Duff's experiments. Duff further infers from investigations by Chabai and Emrich[3] on boundary-layer transition in shock tubes, that the boundary layers would be entirely laminar under the experimental conditions used by him. Furthermore, work by Mirels[7] suggested that in certain cases the boundary layers could be as much as 50% of the channel radius in thickness. This suggests that a considerable portion of the shocked gas is entrained in the boundary layer, and subsequently leaks past the contact surface because of the velocity defect across the boundary layer. In this manner, it is suggested, a considerable amount of the shocked gas mass flow is denied to the region between shock wave and contact surface, so decreasing the effective running time. This mechanism is now firmly established as providing, at least in part, an explanation of the observed dependence of running time on initial channel pressure, channel geometry, and so on. Calculations which rely on this mechanism have been performed by Anderson[4], Roshko[5], Hooker[6], and it is an essential part of the present analysis. All have found at least qualitative agreement between their calculations and experiment. However, quantitatively, previous investigators have not found as good agreement between theory and experiment as would be desired.

In all the analyses, including the present one, the basic physical model assumes a shock wave of constant strength propagating into the stationary gas in the channel. The inviscid core of the shocked gas is assumed to be terminated by a contact surface which remains planar. The analyses are then concerned with estimating the loss of mass flow from the shocked gas region which occurs at the contact surface. The validity of this physical model is discussed later in Section 9 in the light of the available experimental data.

The/

The analyses of Roshko and Hooker are outlined in Section 2, the more important of the restrictions inherent in these analyses being briefly discussed in Section 4 in the comparison between these analyses and the present analysis. The present analysis is developed in Section 3 for both laminar and turbulent boundary layers. Various corrections to the present analysis are outlined in Sections 6 and 7 to account for the effects of the finite bursting time of the diaphragm and turbulent transition in the boundary-layer flow. Hooker's analysis and the present analysis are compared in Section 8 with the experimental data, including the data obtained in the present investigation as outlined in Section 5.

2. A Review of the previous Theoretical Work

Anderson[4] was the first worker to apply boundary-layer theory to the better prediction of shock tube running times. His analysis is confined to the model involving a turbulent boundary layer: this is perhaps valid for normal shock-tube usage where moderately high initial channel pressures are chosen, but most of the experimental results for running time have been obtained with low initial channel pressures and the boundary layer is consequently predominantly laminar. However, he applied his work to only one specific case of a shock of fixed Mach number, travelling into a gas of only one initial channel pressure. Furthermore, we may note that his method is essentially similar to that of Roshko's[5] more general analysis made for a laminar boundary layer.

Roshko's[5] solution is developed to be applicable to all tube geometries, all initial channel pressures, and all shock Mach numbers. However, it does involve some approximations which result in poor quantitative agreement between theory and experiment. Hooker's[6] analysis follows exactly the same method as Roshko's, but adds corrective terms to those obtained by Roshko, thus improving the agreement between theory and experiment. Since the two methods are nearly identical we shall outline Hooker's method, indicating as we proceed the steps at which Hooker's and Roshko's analyses differ.

Referring to Fig. 1, it is seen that Hooker and Roshko have considered the flow relative to contact-surface fixed co-ordinates, the contact-surface velocity in laboratory fixed co-ordinates being assumed to be the ideal value u_2. However, we note that in fact the contact surface moves faster than u_2, as is evident in the running times being shorter than those predicted by ideal-flow theory. This assumption therefore introduces one source of quantitative error between theory and experiment.

Hooker writes the mass-flow rate $\dot{m}_c$ moving past the contact surface via the boundary layer as

$$\dot{m}_c \simeq 2\pi\bar{a}\int_0^{y_{bl}} \rho(y)u(y)dy = 2\pi\bar{a}(\rho_w . u_2 \delta_c^*) \qquad \ldots (2.1)$$

where $\rho(y)$ and $u(y)$ are the density and velocity respectively in the boundary layer, and are functions of the distance from the wall y, y_{bl} denoting the outer edge of the boundary layer. The parameter $\bar{a}$ is the radius (or hydraulic radius) of the channel, whilst suffix w refers to conditions evaluated at the channel walls. The equation (2.1) may be taken to define δ_c^*, the mass-flow thickness of the boundary layer at the contact surface. In obtaining the

integral/

integral term of equation (2.1), Hooker has assumed that $y_{bl}/\bar{a} \ll 1$, and this introduces a second restriction to his model.

Hooker now states that the boundary-layer mass-flow thickness δ_c^* may be obtained by adapting an expression given in Ref. 8 to give

$$\delta_c^* = \beta(\mu_w.\ell/\rho_w.u_2)^{\frac{1}{2}} \qquad \ldots (2.2)$$

where the parameter β is a constant for a particular shock Mach number. The parameter ℓ is the boundary-layer development length up to the contact surface, or the distance at any instant of time between shock wave and contact surface (see Fig. 1).

From expressions (2.1) and (2.2) Hooker shows that β may be written as

$$\beta = \left[f(\zeta_{bl}) - \zeta_{bl}\right] \Big/ \left\{\tfrac{1}{2}\left[\Gamma_{21} - 1\right]\right\}^{\frac{1}{2}} \qquad \ldots (2.3)$$

where ζ is defined by

$$dy = \rho_w \left[2\mu_w x/\rho_w(W_1 - u_2)\right]^{\frac{1}{2}} . \, d\zeta$$

$$u/(W_1 - u_2) = f'(\zeta). \qquad \ldots (2.4)$$

It is to be noted that Γ_{21} is the density ratio across the shock wave whose velocity in laboratory fixed co-ordinates is W_1. The parameter x is the distance behind the shock wave. The function $f(\zeta)$ has been tabulated by Mirels[7], ζ_{bl} being the value of ζ evaluated at the edge of the boundary layer.

Hooker notes that due to an error in transforming from contact-surface fixed co-ordinates to shock fixed co-ordinates, Roshko obtained a different, incorrect expression for β.

Hooker now writes that the mass contained between the shock wave and the contact surface at any instant of time t is

$$m(t) \simeq \pi\bar{a}^2 \rho_2 \ell(t) + 2\pi\bar{a} \int_{x=0}^{\ell(t)} \int_{y=0}^{y_{bl}} \rho(y,x)\,dy.dx \, . \qquad \ldots (2.5)$$

In obtaining the expression (2.5) Hooker again assumes that $y_{bl}/\bar{a} \ll 1$. Roshko neglected the second, integral term in (2.5), which represents the mass contained in the boundary layer between the shock wave and the contact surface.

The rate of change of mass flow between the shock wave and the contact surface, obtained by the differentiation with respect to time of equation (2.5), must be equal to the difference of the mass-flow rate through the shock wave and the mass-flow rate out of the shocked gas region via the boundary layer at the contact surface. Now assuming that at some stage the overall rate of change of mass flow becomes zero, then the boundary-layer development length will have reached a maximum value, $\ell_{max.}$ say, and the running time subsequently will be

constant./

constant. Using the transformation (2.4) Hooker shows that if one writes the boundary-layer development length ℓ as a ratio of $\ell_{max.}$

$$\frac{\ell}{\ell_{max.}} \equiv T \qquad \ldots (2.6)$$

and the time taken, t, for this development as

$$u_2 t \Big/ \left\{ \ell_{max.} \left[\Gamma_{21} - 1 \right] \right\} \equiv X \qquad \ldots (2.7)$$

then X and T may be related by the expression

$$-\tfrac{1}{2}X = \left[\frac{f(\zeta_{bl})}{f(\zeta_{bl}) - \zeta_{bl}} \right] \left\{ \ell n(1-T^{\frac{1}{2}}) + T^{\frac{1}{2}} + \left[\frac{\zeta_{bl}}{2f(\zeta_{bl})} \right] T \right\} \qquad \ldots (2.8)$$

Hooker also shows that the maximum possible boundary-layer development length $\ell_{max.}$ can be expressed as

$$\ell_{max.} = \frac{1}{4\beta^2} \left(\frac{\rho_2}{\rho_w} \right)^2 \frac{\bar{a}^2}{[\Gamma_{21}-1]^2} \cdot \frac{\rho_w u_2}{\mu_w} . \qquad \ldots (2.9)$$

Roshko, in neglecting the integral term mentioned previously, obtained the relation for X and T,

$$-\tfrac{1}{2}X = \ell n(1-T^{\frac{1}{2}}) + T^{\frac{1}{2}} \qquad \ldots (2.10)$$

Roshko, however, obtained the same expression for $\ell_{max.}$.

Hence it is seen that Roshko's expression (2.10) represents a unique curve for X and T, independent of shock Mach number. The dependence on shock Mach number is then only implied in the expressions for $\ell_{max.}$ [equation (2.9)] and X through Γ_{21} [equation (2.7)]. Hooker's expression (2.8), however, represents a set of curves for various shock Mach numbers, since $f(\zeta_{bl})$ etc. are all dependent on shock Mach number.

It is to be noted that the analysis leading to the expression (2.3) for β is based on the assumption that the boundary layer is similar in nature to the flat-plate boundary layer with zero pressure gradient.

It is also seen that although Hooker's analysis is more comprehensive than Roshko's analysis, both methods rely on approximations such that as the boundary layer thickens, these approximations become less valid and tend to lead to overestimates of the running time. This may be seen more clearly by noting that we may write the ratio $\ell/\ell_{max.}$ from (2.2) and (2.9) as

$$\frac{\ell}{\ell_{max.}} = \left(\frac{\delta_c^*}{\bar{a}} \right)^2 . \; 4.T_{21}^2 \; [\Gamma_{21}-1]^2 .$$

Clearly the ratio $\ell/\ell_{max.}$ depends on shock Mach number, and for a shock Mach number of 2 with $\gamma = 5/3$, it is found that as $\ell/\ell_{max.} \to 1$, then

$\delta_c^*/\bar{a}$

$$\frac{\delta_c^*}{\bar{a}} \simeq \frac{1}{5} .$$

However, for a shock Mach number of 6 with $\gamma = 5/3$, it appears that as $\ell/\ell_{max.} \to 1$, then

$$\frac{\delta_c^*}{\bar{a}} \simeq \frac{1}{65} .$$

Consequently it appears that as $\ell \to \ell_{max.}$, the assumption of a thin boundary layer is valid only for high shock Mach numbers. At the lower shock Mach numbers the boundary layer may fill an appreciable part of the channel and one may expect the above analysis to overestimate the running time.

It is more useful to reduce the theoretical results into variables which are readily measured experimentally, i.e. running time in terms of the distance from the diaphragm.

Using the normal shock-wave mass-flow equation

$$u_2 \Gamma_{21} = W_1 (\Gamma_{21} - 1)$$

equations (2.6) and (2.7) may be written as

$$T \equiv \ell/\ell_{max.}$$

$$X \equiv W_1 t/\ell_{max.} \Gamma_{21} . \qquad \ldots (2.11)$$

Referring to Fig. 2, Hooker interprets this as

$$T \equiv \ell/\ell_{max.}$$

$$X \equiv (x' + \ell)/\ell_{max.} \Gamma_{21} \qquad \ldots (2.12)$$

Since $W_1 . t = x' + \ell .$

Also, from the geometry of the (x',t) diagram, Hooker notes that the running time t_R is

$$t_R = \frac{\ell}{W_1} . \qquad \ldots (2.13)$$

This interpretation only assumes that the shock wave has constant speed. Roshko, however, further approximates by obtaining an underestimated value $\bar{\ell}$ for the boundary-layer development length by writing

$$\bar{\ell} = u_2 . t_R .$$

Hence,

$$T \equiv \bar{\ell}/\ell_{max.}$$

$$X \equiv x'/\ell_{max.} \Gamma_{21} .$$

It/

It is seen that the above approximation of Roshko's becomes progressively worse as the contact-surface velocity departs from u_2. This approximation is generally at its worst when the shock Mach number is low, since at the higher shock Mach numbers u_2 approaches W_1, and the error for $\ell \to \ell_{max.}$ is less important. Note that as $\ell \to \ell_{max.}$, according to the analysis, the contact-surface velocity must approach W_1.

For further details of the modifications by Hooker to Roshko's initial analysis, the reader is referred to Ref.6. However, it is briefly noted that the correlation between theory and experiment was greatly improved by Hooker's geometrical interpretations of expressions (2.12) and (2.13), and the retention of the integral term in expression (2.5). Yet even so, the asymptotic approach of $T \to 1$ as $X \to \infty$, or $\ell \to \ell_{max.}$ shows considerable disagreement with experiment for the lower shock Mach numbers. The reasons for this will be discussed in Section 4 where Hooker's analysis is compared with the present analysis.

3. The Present Analysis

3.1 General considerations

If we firstly assume only that the shock wave has constant speed, then referring to Fig. 3, it is seen that as the boundary layer behind the shock grows, the contact surface must accelerate to ensure continuity of mass flow. Writing the contact-surface velocity as u_2', we note that

$$u_2' = u_2'(x',t) \qquad \ldots (3.1.1)$$

and

$$u_2' = u_2 \quad \text{when} \quad x' = t = 0.$$

Consequently, observations at a distance x' from the diaphragm would reveal a running time t_R and the boundary layer behind the shock would have developed to some length x up to the contact surface. Now it follows from the geometry of the (x',t) diagram of Fig. 3, that

$$t_R = \frac{x}{W_1} \qquad \ldots (3.1.2)$$

$$x' = \bar{x} - x.$$

But,

$$\bar{x} = tW_1$$

Hence

$$x' = tW_1 - x. \qquad \ldots (3.1.3)$$

Hence, given any particular distance x' from the diaphragm, in order to find the running time we only require to know the boundary-layer development length x, and the time taken for this development t.

A theoretical approach to the above boundary-layer problem has, in part, been provided by Bernstein[9]. The latter's analysis proceeds by referring to axes at rest relative to the shock, and calculates the boundary-layer

development/

development length in terms of the transformed velocities in the inviscid core of the channel flow. The problem entails modifying the conventional boundary-layer parameters, δ^*, θ, and H for the case of a moving wall. Because of the velocity transformation involved in reducing the shock wave to rest, the walls of the channel are now moving with speed W_1 relative to the shock fixed axes.

3.2 The laminar-boundary-layer running-time analysis

Bernstein shows that for a laminar boundary layer, the development length x may be related to the corresponding local inviscid core flow velocity u_e, by the relationship,

$$\frac{d(x/\bar{a})}{d(u_e/u_{e_o})} = M_{S_1} R_1 T_{12}^{\omega} \; G\left(\frac{u_e}{u_{e_o}}\right). \qquad \ldots (3.2.1)$$

The function $G\left(\frac{u_e}{u_{e_o}}\right)$ is

$$G\left(\frac{u_e}{u_{e_o}}\right) = \frac{\mu_{e_o}}{\mu_e} \cdot \frac{\bar{f}\left(1 - \frac{\rho_e u_e}{\rho_{e_o} u_{e_o}}\right)}{8\bar{H}^2\left(\frac{u_w - u_e}{u_{e_o}}\right)} \times$$

$$\times\left[\left(\frac{\rho_{e_o} u_{e_o}}{\rho_e u_e} - 1\right) \cdot \left(\bar{H} + 1 + \frac{\bar{f}}{6}\frac{\mu_w}{\mu_e} - \frac{u_e/u_{e_o}}{\bar{H}}\frac{d\bar{H}}{d(u_e/u_{e_o})} + M_e^2 - 1\right)\right]. \qquad \ldots (3.2.2)$$

The parameter $\bar{f}$ may be written as

$$\bar{f} = \frac{9{\cdot}072\left[0{\cdot}45 + 0{\cdot}55\frac{T_w}{T_e} + 0{\cdot}09\,(\gamma-1)\,Pr^{\frac{1}{2}} M_e^2\left(\frac{u_w}{u_e} - 1\right)^2\right]^{1-\omega}}{\left(\frac{u_w}{u_e} - 1\right)\left(\frac{u_w}{u_e}\left\{H_i - 1\right\} + 1\right)} \qquad \ldots (3.2.3)$$

and

$$\frac{u_e/u_{e_o}}{\bar{H}}\frac{d\bar{H}}{d(u_e/u_{e_o})} = 1 + (\gamma-1)M_e^2 + \frac{u_w/u_e}{(u_w/u_e)-1}\left[1 - \frac{\bar{H}_i}{\bar{H}}\left(1 + \sqrt{\gamma-1}\, M_e^2\right)\right] - \frac{\bar{H}_i}{H_i}\left(1 - \frac{\gamma-1}{\bar{H}} M_e^2\right). \qquad \ldots (3.2.4)$$

Also note that

$$R_1 = \frac{a_1 \rho_1 \bar{a}}{\mu_1}. \qquad \ldots (3.2.5)$$

Suffix/

Suffix e_o refers to conditions immediately behind the shock wave, and these may be calculated from the normal shock-wave relationships (see Appendix I). Suffix w refers to conditions at the wall, and $\bar{a}$ is the hydraulic radius of the channel.

Referring to the boundary-layer form parameter H, it is to be noted that $\bar{H}$ denotes H evaluated for a moving wall, and suffix i refers to incompressible flow values.

It will be noted that there is no restriction on the boundary-layer thickness, and that although there is no corrective term in the equation (3.2.3) to account for the effects of pressure gradient on $\bar{f}$, the pipe-flow momentum equation which has been solved includes the effects of pressure gradients.

In order to provide a solution to the equations of Section 3.1, we require the time taken for the boundary-layer development to take place, and this may be written as

$$t = \int_o^x \frac{dx}{u_e} . \qquad \ldots (3.2.6)$$

Making use of equation (3.2.1) it follows that

$$t = \frac{\bar{a}}{u_{e_o}} . R_1 M_{S_1} T_{12}^{\omega} \int_1^{u_e/u_{e_o}} \frac{G}{u_e/u_{e_o}} d\left(\frac{u_e}{u_{e_o}}\right) . \qquad \ldots (3.2.7)$$

It also follows from (3.2.1) and (3.2.7) that

$$\frac{x}{R_1 \bar{a}} = M_{S_1} T_{12}^{\omega} \int_1^{u_e/u_{e_o}} G . d\left(\frac{u_e}{u_{e_o}}\right) \qquad \ldots (3.2.8)$$

and

$$\frac{t . u_{e_o}}{R_1 \bar{a}} = M_{S_1} T_{12}^{\omega} \int_1^{u_e/u_{e_o}} \frac{G}{u_e/u_{e_o}} . d\left(\frac{u_e}{u_{e_o}}\right) . \qquad \ldots (3.2.9)$$

Now although t is the actual time for the boundary layer to develop to a length x, u_{e_o} remains the gas velocity relative to the shock wave. Hence,

$$u_{e_o} = w_1 - u_2$$
$$= (M_{S_1} - U_{21}) a_1 .$$

It is shown in Appendix I, equation (A.1.1), that

$$\frac{u_{e_o}}{a_1} = \frac{\frac{\gamma-1}{2} M_{S_1}^2 + 1}{\frac{\gamma+1}{2} M_{S_1}} . \qquad \ldots (3.2.10)$$

We/

We may now make equations (3.1.2) and (3.1.3) non-dimensional for use with equations (3.2.8) and (3.2.9) so that

$$\frac{x'}{R_1\bar{a}} = \frac{tw_1}{R_1\bar{a}} - \frac{x}{R_1\bar{a}} = \frac{t.u_{e_0}.M_{s_1}}{R_1\bar{a}} \cdot \frac{a_1}{u_{e_0}} - \frac{x}{R_1\bar{a}}$$

and

$$\frac{t_R}{R_1\bar{a}} = \frac{x}{R_1\bar{a}} \cdot \frac{1}{W_1} .$$

Hence,

$$\frac{t_R a_1}{R_1\bar{a}} = \frac{1}{M_{s_1}} \cdot \frac{x}{R_1\bar{a}} .$$

Equations (3.2.8) and (3.2.9) have been integrated numerically on the University of London 'Mercury' Computer to give:

$$\frac{10^4 x}{R_1\bar{a}} \equiv X \qquad \ldots (3.2.11)$$

$$\frac{10^4 t.u_{e_0}}{R_1\bar{a}} \equiv T \qquad \ldots (3.2.12)$$

$$T \cdot \frac{a_1}{u_{e_0}} \cdot M_{s_1} - X \equiv X' \qquad \ldots (3.2.13)$$

$$\frac{X}{M_{s_1}} \equiv T_R . \qquad \ldots (3.2.14)$$

All these non-dimensional parameters, X, X', T, and T_R are evaluated as functions of u_e/u_{e_0} and X' and T_R are plotted in Figs. 4a and 4b for $\gamma = 7/5$ and $\gamma = 5/3$.

In the evaluation of R_1 for the reduction of experimental data and the prediction of the running time from theory it must be remembered that

$$R_1 = \frac{a_1 \rho_1 \bar{a}}{\mu_1}$$

$$= \frac{a_1}{\mu_1}\frac{\rho_s}{p_s} \cdot p_1\bar{a}$$

$$= \left(\frac{a}{\mu} \cdot \frac{\rho}{p}\right)_s p_1 .\bar{a} \qquad \ldots (3.2.15)$$

where/

where suffix s refers to room temperature conditions, and p_1 is the initial channel pressure.

3.3 The turbulent-boundary-layer running-time analysis

In his turbulent-boundary-layer analysis, Bernstein[9] deduced a similar relationship to (3.2.1) for x and u_e.

$$\frac{d(x/\bar{a})}{d(u_e/u_{e_o})} = \left[R_1 M_{s_1} T_{12}^{\omega}\right]^{2/(n+1)} \cdot F\left(\frac{u_e}{u_{e_o}}\right). \qquad \ldots (3.3.1)$$

The function $F\left(\frac{u_e}{u_{e_o}}\right)$ is

$$F\left(\frac{u_e}{u_{e_o}}\right) = \frac{u_{e_o}}{u_e}\frac{1}{2J\bar{H}}\left\{\frac{1-(\rho_e u_e/\rho_{e_o}u_{e_o})}{2\bar{H}(\mu_e/\mu_{e_o})}\right\}^{2/(n+1)} \times$$

$$\times\left[(M_e^2-1)+\left(\frac{\rho_{e_o}u_{e_o}}{\rho_e u_e}-1\right)\left(\bar{H}+1-\frac{u_e/u_{e_o}}{\bar{H}}\frac{d\bar{H}}{d(u_e/u_{e_o})}\right)\right]. \qquad (3.3.2)$$

The parameter J may be written as

$$J = \left\{\frac{n+(2u_w/u_e)}{C^n(n+1)(n+2)}\cdot\frac{\mu_w}{\mu_e}\right\}^{2/(n+1)}\cdot\frac{\rho_m}{\rho_e}\left(\frac{u_w}{u_e}-1\right)^2. \qquad (3.3.3)$$

Again $\frac{u_e/u_{e_o}}{\bar{H}}\frac{d\bar{H}}{d(u_e/u_{e_o})}$, and R_1 are given in (3.2.4) and (3.2.5).

Proceeding in the same manner as Section 3.2, it can be shown that

$$\frac{10^4\, t\, u_{e_o}}{R_1^{2/(n+1)}\bar{a}} = 10^4\left[M_{s_1}T_{12}^{\omega}\right]^{2/(n+1)}\cdot\int_1^{u_e/u_{e_o}}\frac{F}{u_e/u_{e_o}}\cdot d\left(\frac{u_e}{u_{e_o}}\right) \equiv T \qquad \ldots (3.3.4)$$

and

$$\frac{10^4 x}{R_1^{2/(n+1)}\bar{a}} = 10^4\left[M_{s_1}T_{12}^{\omega}\right]^{2/(n+1)}\cdot\int_1^{u_e/u_{e_o}} F\cdot d\left(\frac{u_e}{u_{e_o}}\right) \equiv X. \qquad \ldots (3.3.5)$$

Similarly, we now define

$$\frac{10^4 x'}{R_1^{2/(n+1)}\bar{a}} = T\cdot\frac{a_1}{u_{e_o}}\cdot M_{s_1} - X \equiv X' \qquad \ldots (3.3.6)$$

$$\frac{10^4 t_R a_1}{R_1^{2/(n+1)}\bar{a}} = \frac{X}{M_{s_1}} \equiv T_R. \qquad \ldots (3.3.7)$$

The/

The index n occurs throughout these equations since Bernstein assumes a power-law velocity profile throughout the boundary layer. Although the usual power-law assumption for steady flow is $n = 7$, work by Martin[10] suggests that $n = 5$ may be a better approximation for the quasi-steady shock-tube turbulent-boundary-layer problem. Consequently, equations (3.3.4) and (3.3.5) have been integrated numerically using both power-law assumptions. The constant c in equation (3.3.3) is dependent on n, and has been taken to be 6·20 for $n = 5$ and 8·74 for $n = 7$. A recovery factor of 0·89 has also been assumed in calculating the density at the mean enthalpy, ρ_m, and the power-law temperature, viscosity relationship has been used so that $\omega = 0{\cdot}76$.

The results of equations (3.3.6) and (3.3.7) are plotted in Figs. 5a-d, for $\gamma = 7/5$ and $\gamma = 5/3$.

4. A Comparison of the Present Analysis and Hooker's Analysis

Both the present analysis, assuming a laminar boundary layer, and Hooker's analysis have been calculated for specific heat ratios of $\gamma = 7/5$ and and $\gamma = 5/3$. The two analyses are compared in Figs. 4a and 4b in terms of the non-dimensional running time T_R and the corresponding non-dimensional distance from the diaphragm X' used in Section 3.2.

It is immediately evident that for the low shock Mach numbers there is considerable disagreement in the values of the asymptotes of T_R between the two analyses. For example, taking the extreme case of $M_{s_1} = 1{\cdot}6$ and $\gamma = 5/3$ (Fig. 4b) it is seen that the asymptotic value of T_R according to Hooker's analysis is 2470, whereas the present analysis predicts an asymptote of nearly one tenth of this value. Furthermore, the approach by X' to the asymptote is much more rapid in the present analysis. However, as the shock Mach number increases, it is seen that the disagreement between the two theories decreases.

The reasons for the varying discrepancies between the two analyses appear to be twofold. Firstly, it must be noted that in order to produce the maximum possible running time, the inviscid core flow velocity must increase from the ideal value of u_2 immediately behind the shock wave until the contact surface is moving with the speed of the shock wave W_1. This velocity increase can be shown to be strongly dependent on shock Mach number. For example, for a shock Mach number of 1·6, with $\gamma = 5/3$, the fractional velocity change $(W_1 - u_2)/u_2$ required to produce a maximum possible running time is 1·12, whereas for a shock Mach number of 6, with $\gamma = 5/3$, the fractional velocity change is only 0·37. This suggests that for the higher shock Mach numbers, Hooker's analysis, relying as it does on the assumption that only small changes in flow parameters occur, is more in keeping with the physical model. The second point is that already mentioned in Section 2, where it is shown that at the higher shock Mach numbers the boundary layer occupies a much smaller portion of the channel. Here again, Hooker's assumption of a thin boundary layer is more appropriate to the physical model than it is for the lower shock Mach numbers where the boundary layer is seen to be thick.

It is to be noted that otherwise the basic physical models for the present analysis and the Roshko-Hooker analysis are very similar. In both analyses a constant strength shock wave is assumed, generating a quasi-steady boundary layer. However, the subsequent exercise then demands satisfying the mass-flow equation in the shocked gas region and also the momentum equation. Bernstein's[9] analysis in fact solves these two equations simultaneously, providing a solution which gives the variation of the inviscid core flow velocity u_e with the boundary-layer development length x. The present analysis is then concerned with calculating the time required for this

development/

development to take place [cf. equation (3.2.6)]. The Roshko-Hooker analysis on the other hand only satisfies the mass flow equation, and in an approximate form. The Bernstein analysis, however, does involve the assumption that the value of the boundary-layer form parameter, H, may be taken to be the flat-plate value, the argument being that H is insensitive to small variations in velocity profile. With the small pressure gradients involved this assumption is not likely to introduce significant errors.

The turbulent-boundary-layer analysis, obtained from equations (3.3.6) and (3.3.7), is plotted in Figs. 5a - d, for $\gamma = 7/5$ and $\gamma = 5/3$. The turbulent-boundary-layer analysis cannot be compared with either the present laminar-boundary-layer analysis or the Roshko-Hooker analysis in the X', T_R plane since the parameter R_1 in the turbulent analysis is raised to the power $2/(n+1)$.

It must be noted that although the behaviour of the steady compressible laminar boundary layer is now fairly well understood, the behaviour of the turbulent boundary layer is not so well defined. Consequently the use of Bernstein's turbulent-boundary-layer analysis used in Section 3.3 is open to question, and the reader is directed to Bernstein's paper[9] for further discussion on this topic.

5. The Present Experimental Work

5.1 The apparatus

The channel of the shock tube used in the present investigation is 16 feet long and $1\frac{1}{2}$ inches square in internal cross-section. The channel has 11 possible measuring stations situated $1\frac{1}{2}$ feet apart which normally contain barium titanate shock-wave detectors. The output from these detectors could be fed via thyratron trigger amplifiers to a Rank-Cintel decimicrosecond chronometer and a Tektronix oscilloscope.

The driver used was 4 feet long and 3 inches i.d. in section, the driver pressures being measured with two Budenberg standard test gauges, one reading 0(2)400 p.s.i. gauge, the other reading 0(50)2000 p.s.i. gauge. The vacua used in the channel were measured with two Wallace and Tiernan absolute pressure gauges, one reading 0(0.5)100 mm Hg, the other reading 0(2)800 mm Hg. For readings at high vacua an Edwards Pirani gauge was provided. All the vacuum gauges were calibrated against an oil manometer.

The contact-surface detectors used in the investigation were those described by Bernstein[12], and were simply glass rods with thin platinum films baked onto the leading edges, and could be placed in any of the 11 measuring stations. The films were supplied by constant current sources, the voltage change produced by the heating of the platinum, when the shocked gas impinged upon it, being fed through amplifiers to the oscilloscope.

The diaphragm material used was Melinex, the diaphragm being shattered by a plunger operated by a simple pawl mechanism.

5.2 The experimental results

All the running-time measurements were carried out in nitrogen, the driver gas being hydrogen in the case of the $M_{s_1} \simeq 6$ runs, and nitrogen for the $M_{s_1} \simeq 3$ runs. It was felt that the initial shock Mach number measured near to the diaphragm might have more significance in the correlation with theory than would the local shock Mach number.

Measurements/

Measurements near the diaphragm were first obtained as a check that the initial shock Mach number was close to either 3 or 6. Once the channel and driver pressures were found to produce these initial shock Mach numbers they were used throughout the subsequent experiments for the particular initial channel pressure selected.

The raw results are presented in Figs. 6 - 9. It will be noted that there is some scatter in the results, probably due to small variations in driver and channel pressures and a varying quality in the bursting of the diaphragms. The latter effect was minimised by discounting results where it was seen that the diaphragm had not petalled cleanly. Since the more accurate Wallace and Tiernan gauge was sensitive to $\frac{1}{3}$ mm Hg pressure changes, the varying pressure effects were difficult to eradicate.

A limitation was imposed on the minimum channel pressure possible for experimental measurements because of triggering difficulties. For a particular shock Mach number the size of the pulse given out by the barium titanate transducers is proportional to the initial channel pressure. Consequently at the lowest pressures used (0.7 mm Hg) the sensitivity of the trigger amplifiers was at a maximum, and the thyratrons then tended to be triggered by stress waves in the channel walls due to the bursting diaphragm, rather than by the shock wave.

6. A Correction for the Finite Bursting Time of the Diaphragm

It is known[11] that the primary shock wave is not instantaneously generated at its full strength when the diaphragm begins to open. A consequence of the finite bursting time of the diaphragm is that the shock wave accelerates to approximately the strength indicated by simple theory through a series of coalescing compression waves generated at successive stages of the diaphragm's opening. A further consequence is that the contact surface accelerates from rest over some finite time dependent on the diaphragm opening time. This process is illustrated in Region A of Fig. 11. It is noted that in this region there is considerable departure from the physical model used for the description of running-time variations. This indicates that there might be some discrepancy between the analysis and experiment at some small distance from the diaphragm. This, in fact, appears to be so, since the experimental curves of running-time distribution along the channel of Figs. 6 - 9 show no indication that the experimental curve, if smoothly extrapolated, would pass through the origin.

Now if it is assumed that the shock wave and contact surface position themselves in the (x',t) diagram without influence from the boundary layers also generated in this process (this is reasonable since the whole flow field is rapidly accelerating so that the boundary layers will be thin), then some correction may be made to the analysis to allow for the finite bursting time of the diaphragm.

It is seen from Fig. 11 that the model of the flow used in the prediction of running time has an origin at O'. Here the shock-wave and contact-surface trajectories, as observed at some station B, have been extrapolated according to the present analysis to the point O'. In other words, on the basis of the measured running time at station B, the physical model gives the origin of the shock wave and contact surface as being some distance, $(x'_A + OB)$, from B. Consequently, it has been the practice in the experiments carried out in the present investigation to measure the running time at some position close to the diaphragm (but where the measured shock Mach number is that predicted by simple theory, thus avoiding misleading running-time measurements in region A), and then from the analysis of Section 3.2, calculating $(x'_A + OB)$.

Hence/

Hence once x'_A is known, it may then be applied to the predictions of running time further along the channel. It is to be noted that x'_A should remain constant, or nearly so, for one particular initial pressure in driver and channel, and one particular diaphragm thickness, provided the diaphragm always bursts in the same clean manner.

It is to be noted that the correction x'_A may be positive or negative as required, and that the method outlined above will subsequently be referred to as laminar-boundary-layer analysis matching.

7. The Matching of Laminar- and Turbulent-Boundary-Layer Running-Time Analyses

The analyses given in Sections 3.2 and 3.3 are based on boundary layers which are either laminar or turbulent. It is of interest to examine the effect on running time of transition to turbulent boundary-layer flow, since transition may have a marked effect on the running-time distribution along the channel.

On the assumption that at some point in the growth of the laminar-boundary-layer transition occurs, and subsequently moves with the shock velocity, it is possible to match the two running-time analyses at the first occurrence of transition, and compute the subsequent analytical running-time distribution along the channel.

An appeal to the quasi-steady flow model of Fig. 12a, where the shock is at rest, shows that the inviscid core velocity, u_e, is the same at either side of the transition point τ, and that the virtual development length of the turbulent boundary layer is a distance x_T ahead of transition.

Examining the (x',t) plane of Fig. 12b, it is evident that there must be continuity of running time through the transition point. That is to say that the first particle set in motion by the shock wave experiences transition at τ and until then it has been at the extremity of a growing laminar boundary layer; subsequently its trajectory is controlled by the growing turbulent boundary layer. Consequently the contact surface describes the path $\vec{C_L}$ until the point τ is reached, whereafter the contact surface describes the path $\vec{C_T}$. It is also evident from Fig. 12b that the virtual origin of the turbulent boundary layer is at O_T, a distance x'_T ahead of τ. (The reader is here asked to note that the various symbols used in the subsequent argument are defined in Fig. 12).

Assuming that the distance of the initial transition point τ from the diaphragm is x'_τ and is known, then the running time, t_R, at that point is also known together with the corresponding value of u_e/u_{e_0}. Consequently x'_T and t_{R_τ} may be calculated from the turbulent-boundary-layer analysis, remembering that the value of u_e/u_{e_0} is conserved through the transition point τ. Hence the time t_1 can now be calculated since

$$t_1 = t_R - t_{R_\tau} . \qquad \ldots (7.1)$$

With the assumption that the subsequent transition point remains at a constant distance behind the shock wave, then it follows that t_1 remains constant for the remainder of the (x',t) diagram, if the shock is assumed to have a constant speed throughout its motion. Now the turbulent-boundary-layer analysis may then be used to calculate the running time $t_{R(TURB)}$ behind a 'virtual' shock '$\vec{S}$' at some distance $x'_{(TURB)}$ from O_T. Consequently the actual running time t_{R_1} experienced at some distance, x'_1, from the diaphragm is now

t_{R_1}/

$$t_{R_1} = t_1 + t_{R(TURB)} \qquad \ldots (7.2)$$

and the actual distance, x_1', from the diaphragm is given by

$$x_1' = x'_{(TURB)} - x_T' + x_\tau' \ . \qquad \ldots (7.3)$$

Again in this problem it is necessary to apply a correction for the finite bursting time of the diaphragm as outlined in Section 6, so that the relationship (7.3) may be modified to give

$$x_1' = x'_{(TURB)} - x_T' + x_\tau' \pm x_A' \ . \qquad \ldots (7.4)$$

The decision as to where the transition point, if any, first occurs in the experimentally obtained running-time distribution along the channel is sometimes difficult to make. However, the running-time distributions shown in Figs. 6 and 8 show quite striking departures from the predictions of the laminar boundary-layer analysis, even when matched at the first experimental point. These departures seem to be much greater than could be expected due to shock attenuation, and indeed the measured values of shock Mach number, for the experimental points subsequent to the initial departure of experiment from the analysis, show no rapid attenuation of the shock wave in this region. Consequently the most likely reason appears to be the occurrence of transition. Furthermore transition Reynolds numbers (see Appendix II) calculated on the assumption that transition in fact does occur at the point of departure agree quite well with transition Reynolds numbers found by other investigators[5].

8. A Comparison of the Analyses with Experiment

The running-time distributions along the channel obtained in the present investigations, using nitrogen in the channel, are plotted in Figs. 6 - 9. All the analytical curves included in the comparison have been matched to the first experimental points in accordance with the method of Section 6. It is to be noted that generally the experimental points compare favourably with the present analysis, but that there are, in some cases, marked differences between the laminar-boundary-layer analysis and experiment, even when allowances have been made for the finite bursting time of the diaphragm.

In the case of $M_{S_1} \simeq 3{\cdot}0$ and $p_1 = 5{\cdot}6$ mm Hg (Fig. 6) it is seen that there appears to be no increase in running time after approximately 8 feet of the channel has been traversed by the flow. As has been argued in Section 7, the most likely explanation of this is that transition has occurred in the boundary layer. On this assumption the modified analytical curve 'to the right' of the point τ, which indicates the assumed transition point, has been prepared using the method of Section 7. The agreement between experiment and the modified analysis allowing for transition is seen to be greatly improved. Furthermore, the transition Reynolds number $\bar{R}_\tau$ calculated for the assumed transition point (see Appendix II) is of the order to be expected.

The results for $M_{S_1} \simeq 3{\cdot}0$ and $p_1 = 3{\cdot}3$ mm Hg (Fig. 7) show some discrepancy with the present laminar-boundary-layer analysis at about 13 feet from the diaphragm and calculations show that it is possible that transition has also occurred at this point.

In the case of $M_{S_1} \simeq 6{\cdot}0$ and $p_1 = 5$ mm Hg (Fig. 8) the interpretation is a little complicated by shock attenuation. A crude allowance has been made for this by simply deducting from the present laminar-boundary-layer analysis

the/

the time between the arrival of the measured shock-wave trajectory and the constant shock-wave trajectory postulated in the physical model (see Fig. 15). This is essentially a linearisation of the problem and more will be said of this later. Transition has also been assumed at τ, and the comparison between the modified analysis and experiment is seen to be good.

The remaining results for $M_{s_1} \simeq 6{\cdot}0$, that is for values of p_1 of 3·5 mm Hg and 1·2 mm Hg (Fig. 9), show considerable scatter and general disagreement with the matched laminar-boundary-layer analysis. It is felt that the general disagreement with the analysis may be due to shock attenuation, and the scatter to inaccurate initial pressures and poor diaphragm bursts (very thin diaphragms were used in these particular runs and did not petal cleanly).

All the results obtained in the present investigation are plotted in the X', T_R plane of Fig. 10a, and compared with the results of the present laminar-boundary-layer analysis and Hooker's analysis. Poor agreement is to be noted for the $M_{s_1} \simeq 6{\cdot}0$ results, but for $M_{s_1} \simeq 3{\cdot}0$ the agreement is seen to be good for both analyses. The experimental points at the region where the two analyses begin to depart from one another tend to follow the predictions of the present analysis.

Duff[2] has measured the running time along a shock-tube channel of radius 1·43 cm. He used argon as the channel gas at an initial pressure of 0·5 mm Hg. The driver pressure was adjusted for each experiment so that the shock Mach number obtained at the measuring station (the local shock Mach number) was 1·6. His results are plotted in the X', T_R plane of Fig. 10b, and it is seen that the agreement with the present laminar-boundary-layer analysis is good, whereas Hooker's analysis predicts running times vastly greater than Duff's results. Besides the measurements noted above, Duff also examined the dependence of running time on initial channel pressure. He measured the running time at a constant distance of 3·81 metres from the diaphragm, and kept the local shock Mach number near to 1·6 by adjusting the diaphragm pressure ratio. His results are plotted in Fig. 13b, in the $t_R/t_{R_{TH}}$, p_1 plane (they are also included in the X', T_R plane of Fig. 10b) together with the predictions of the present laminar-boundary-layer analysis and Hooker's analysis for shock Mach numbers of 1·6 and 2·0. The experimental results are seen to be in close agreement with the present analysis for a shock Mach number of 1·6. Note that as Hooker points out, the curves of $t_R/t_{R_{TH}}$ against p_1 are not strongly dependent on shock Mach number.

Duff carried out a third set of experiments in which he measured the running time at 3·81 metres from the diaphragm using a constant initial channel pressure of 0·5 mm Hg with argon as the channel gas. In these experiments the local shock Mach number was varied, the results being plotted in Fig. 14a. Here again good agreement is obtained with the predictions of the present laminar-boundary-layer analysis.

Hooker's results[6] obtained in argon are presented in the X', T_R plane of Fig. 10c. He measured the running time at 6·27 metres from the diaphragm in a channel whose diameter was 3·95 cm, and covered a wide range of pressures and local shock Mach numbers. The points plotted in Fig. 10c have against them the measured local shock Mach number, and it is seen that it is difficult to correlate these points with the analytical curves. When re-plotted in the $t_R/t_{R_{TH}}$, p_1 plane of Fig. 13a they tend to collapse onto a mean curve, and in general agree reasonably well with the present analysis for $M_{s_1} = 4{\cdot}0$. The slight dependence of the analyses on shock Mach number is here even more striking.

Hooker/

Hooker provides experimental results where the initial channel pressure is greater than 5 mm Hg, but these results show considerable disagreement with the analyses. It is felt that these results represent conditions in which a partly turbulent boundary layer is existent, and consequently the $t_R/t_{R_{TH}}$, p_1 plane has not been extended to include them.

Appleton and Musgrove[19] have measured the dependence of running time on initial channel pressure using air as the channel gas. The channel radius was 1·77 in. and measurements were made at a distance of 6·32 ft from the diaphragm. The local shock Mach number was arranged to be 5·0 for each experiment, and the results are plotted in Fig. 13c. It is to be noted that there is some discrepancy between the analyses and experiment. A possible explanation is that the diaphragm opening times were large, and this might produce marked effects on measurements taken so close to the diaphragm.

A second set of experiments performed by Appleton and Musgrove consisted of measuring the variation of running time with shock Mach number. The initial channel pressure was 50 mm Hg, and the results are presented in Fig. 14b, together with the predictions of the present laminar- and turbulent-boundary-layer running-time analyses. It is seen that the experimental points fall between the two at the lower shock Mach numbers, but begin to agree with the turbulent-boundary-layer analysis with $n = 5$ as the shock Mach number increases. The Reynolds number $\bar{R}$ has been calculated assuming that the boundary-layer development length up to the contact surface x may be obtained from the laminar-boundary-layer analysis of Bernstein (see Section 3.2). It is seen that $\bar{R}$ is not much greater than the usual values to be expected of the transition Reynolds number $\bar{R}_T$ when $M_{S_1} = 2{\cdot}0$. Consequently it is possible that a significant part of the boundary layer is still laminar when $M_{S_1} = 2{\cdot}0$, and so the actual running time might be expected to have a value somewhere between the predictions of the laminar- and turbulent-boundary-layer analyses. It is to be noted that as the shock Mach number increases, so the value of $\bar{R}$ increases. One might then expect the extent of the laminar boundary layer to decrease. On this basis it appears that the actual running time should therefore tend to the predictions of the turbulent-boundary-layer analysis as the shock Mach number increases, and this, in fact, is the case.

It should be noted that the predictions of the turbulent-boundary-layer analysis with $n = 5$ appear to fit the existing data better than the predictions where $n = 7$. Also the running time does not appear to depend on the driver gases used.

9. A Discussion on the Validity of the Physical Model

The simplified physical model of the flow used in all the analyses assumes a shock wave of constant speed, and also that the contact surface remains a surface of discontinuity. That these assumptions are not generally true is well known; the shock-wave attenuates due to the boundary-layer growth[12], and the contact surface, if it ever exists as such, rapidly spreads into a highly turbulent mixing region. Consequently, to provide an exact description of the flow that exists in the shock tube, we should be obliged to solve the shock-wave attenuation problem and determine how far, if at all, the contact region extends into the shocked gas flow. The solutions to the first problem of shock-wave attenuation, all based on linearisation methods, are discussed by Bernstein[9,12]. A solution to the problem of contact surface spread has been provided by Hall[13], again using a linearisation technique, assuming that the density difference across the contact surface is small. Neither the solutions to the shock-wave

attenuation/

attenuation problem, nor Hall's solution to the contact-surface mixing problem compare well with the experimental evidence, except at very low shock Mach numbers.

The problem of shock-wave attenuation coupled to the prediction of running time is a difficult problem to formulate, in that one requires to know how quickly the boundary layer, particularly at the head of the contact region, responds to changes in shock strength. A method for accounting for shock-wave attenuation, which ignores the above point, has been described previously in Section 8, so that this method is very difficult to justify fully although it provides a reasonable correction to the analysis in the case considered. It should be noted that good agreement with experiment could be obtained by simply ignoring the shock-wave attenuation effect and assuming that transition occurred rather earlier (see Fig. 8). The method used to account for shock-wave attenuation is based on the assumption that it will take some time for the effect of the changing shock speed to reach the boundary layer at the contact surface. The sketch of Fig. 15 explains what has been done. Time is deducted from the predictions of the present running-time analysis, the time deducted being the time between the arrival at a particular station of the ideal constant-speed shock wave, and the arrival at the same station of the shock wave of known measured speed. This method seems to provide an adequate small correction to the present analysis in the case of $M_{S_1} = 6{\cdot}0$, $p_1 = 5$ mm Hg in nitrogen (Fig. 8). However, the above argument appears to be of very doubtful validity in the case of Duff's experimental data[2]. Duff measured the running-time distribution along the channel, but arranged the driver pressure so that at whichever station he measured the running time, the local shock Mach number was 1·6. Duff shows in his paper that the shock Mach number near the diaphragm was often much higher than 1·6; in fact it was of the order of 2. An attempt to correct the present running-time analysis for this large amount of shock-wave attenuation led to very much smaller running times than Duff's data shows. Consequently, one is forced to the conclusion that either the present analysis is inaccurate in its predictions, or that the boundary layer at the contact surface rapidly responds to changes in shock speed in the circumstances of these particular experiments. One possible argument is that in the inviscid core of the flow, the feedback of information concerning the changing shock speed passes along the negative characteristics; the velocity of the information is $(u-a)$. Now if the shock Mach number is high then the slope of such characteristics is high, since the Mach number of the shocked gas flow increases with increase of the shock Mach number. However, if the shock Mach number is low the slopes of the $(u-a)$ characteristics are smaller and here one might expect more rapid conveyance of information to the contact region of details of changes of shock speed. The above argument does not indicate, however, how quickly the boundary layer reacts to changes in external flow conditions and this is clearly important. Consequently, it would be of considerable interest to perform experiments not only in which the running-time distribution along the channel would be measured, but also the shock-wave attenuation. In this manner an (x',t) diagram could be constructed which might reveal the response of the contact surface to changes in shock speed.

The problem of contact-surface mixing may be soluble by means of the classical turbulent transport theory. There is a change in momentum across the contact region because of the change in density occurring there, so that one may be able to show that there is a continuous change in mean density through the contact region, and that the turbulent region will spread. It has been suggested[14] that the problem of contact-surface spread may be explained in terms of Taylor's analysis[15] of the instability of discontinuities such as the contact surface. Yet considering the large amount of turbulence generated

by/

by the bursting diaphragm it seems unlikely that a contact surface is even initially formed and that the disturbances initially present in the flow may be regarded as small, so that conditions for Taylor instability hardly seem to arise.

There remain two further points worthy of mention concerning the validity of the assumed physical model. The first is that the model discounts any effects due to the presence of the cold driver gas. That the driver gas does effect shock-wave attenuation is known[9]. Consequently one might expect to notice variations in running time due to the use of different driver gases. This may in part explain the rather poorer correlation between the present analysis and experiment in the case of the $M_{s_1} \simeq 6{\cdot}0$ runs performed in the present investigation. In the latter experiments hydrogen was used as the driver gas, whereas with the $M_{s_1} \simeq 3{\cdot}0$ runs, using nitrogen as the driver gas, the correlation between the present analysis and experiment was seen to be generally good. In this respect it has been noted in Section 8 that the results of Appleton and Musgrove (Fig. 14b) show no such dependence of running time on the driver gas. However, only helium and air drivers were used, whereas the use of hydrogen as the driver gas is known[9] to have a much more marked effect on shock-wave attenuation than helium.

The second point is that, in the present analysis, real-gas effects have been entirely ignored. This is a reasonable assumption provided that the shock Mach number is lower than, say, $M_{s_1} = 6$ but as is mentioned in Section 1, Henshall[1] shows that at higher shock Mach numbers real-gas effects cannot be ignored. It is to be noted that both Roshko[5] and Hooker[6] partially deal with the presence of real gases by the incorporation of a compressibility factor in the equation of state.

A modification to the present analysis to include real-gas effects is possible. A first approximation would be simply to calculate the condition of the gas immediately behind the shock wave, using the real-gas tables calculated by, say, Bernstein[16]. Thereafter the variation of the gas parameters in the inviscid core of the flow might be calculated assuming the simple ideal-gas isentropic flow equations, but using a value of γ appropriate to the conditions already calculated immediately behind the shock wave. Furthermore, a second approximation might be effected, taking into account variations in the atomic structure of the molecules in the inviscid core of the flow. However, the inclusion of real-gas effects in the description of the boundary layer itself, together with the above approximations, would certainly make the resulting running-time problem exceedingly cumbersome. The possibility of solution to this latter problem, however, would seem to depend as much on the size and speed of existing computing machines as on any lack of knowledge of the behaviour of real-gas flows.

10. Concluding Remarks

It has been shown that the 'linearisation' methods of the previous analyses used to predict shock-tube running times are no longer adequate when the boundary layers are thick relative to the channel radius. An alternative analysis has been demonstrated which does not include some of the more restrictive assumptions of the previous analyses, and gives results in better agreement with the experimental data. Corrections are explained to account for the remaining discrepancies between the present analysis and experiment in terms of turbulent transition in the boundary layer, and the finite bursting time of the diaphragm. The correlation of the present analysis with experiment is then shown to be much improved.

It/

It is suggested that further work be carried out to show the dependence of the contact-surface trajectory on the attenuation of the shock wave. Also, it is suggested that the structure of the contact region be examined in detail.

As is noted in Section 9, the driver gas may have some effect on the duration of running time, so that it may be worth while examining experimentally the effect of using different gases, particularly hydrogen, to produce shocked gas flows having identical initial conditions.

The variation of running time might also be examined experimentally at high shock Mach numbers where real-gas effects begin to be appreciable. At the same time the present analysis of Section 3 might also be repeated to include the kind of real-gas approximations outlined in Section 9.

Since little experimental data are available on running times where it is known that the boundary layer is entirely turbulent, it would be of interest to perform experiments in which the boundary-layer flow conforms to this condition.

Finally it is perhaps worth reiterating Hooker's point that since the running times in shock tubes can be considerably less than the predictions of simple theory, the usual gas parameters of the inviscid core of the shocked gas flow can be far from constant. Therefore care should be observed in the interpretation of the experimental results so that the constancy of these gas parameters is not necessarily taken for granted.

Acknowledgments

Thanks are due to Dr. L. G. Whitehead for his help and interest in the design and construction of the apparatus used in the present experimental investigation. To Dr. L. Bernstein the author wishes to make known his gratitude for the many useful discussions concerning practical and theoretical matters. Thanks are also due to Mr. W. H. Montague who built much of the apparatus, particularly in the construction of the vacuum systems. Finally, the author would like to thank Professor A. D. Young for his interest, encouragement, and many helpful comments in the preparation of this paper.

---

11. Notation

a_i	speed of sound in region i
A_{ij}	speed of sound ratio a_i/a_j
$\bar{a}$	hydraulic radius of channel = 2 × area/perimeter
$\vec{C}$	contact-surface trajectory
c	constant relating to the turbulent-boundary-layer velocity-distribution power law
F	function defined by equation (3.3.2)
$\bar{f}$	parameter defined by equation (3.2.3)
G	function defined by equation (3.2.2)
H, H_i	boundary-layer form parameters in stationary wall case - suffix i denotes incompressible flow
$\bar{H}$, $\bar{H}_i$	boundary-layer form parameters in moving wall case - suffix i denotes incompressible flow
J	parameter defined by equation (3.3.3)
ℓ	distance between shock wave and contact surface
M	Mach number
m	mass flow
$\dot{m}$	mass-flow rate
n	index in turbulent boundary-layer power-law velocity profile
P_r	Prandtl number
p_i	pressure in region i
R	Reynolds number
$\vec{S}$	shock wave trajectory
T_i	temperature in region i
T_{ij}	temperature ratio T_i/T_j
T	non-dimensional time
t	time
u	velocity
u_i	velocity in region i

U_{ij}'

U_{ij} velocity ratio u_i/u_j

W_i wave speed into region i

w distance covered to transition point

X non-dimensional distance

x boundary-layer development length, including the development length up to the contact surface

y distance from wall of channel

β constant defined by equation (2.3)

γ specific heat ratio

Γ_{ij} density ratio ρ_i/ρ_j

δ^* boundary-layer displacement thickness

θ boundary-layer momentum thickness

ζ function defined by equation (2.4)

μ_i dynamic viscosity in region i

ρ_i density in region i

τ transition point

$\vec{\tau}$ transition-point trajectory

ν_i kinematic viscosity in region i

ω index used to define dependence of viscosity on temperature.

Suffices

1 refers to quantities in region ahead of primary moving shock wave

2 refers to quantities in region immediately behind primary moving shock wave

o refers to conditions immediately behind stationary shock wave

A refers to corrections resulting from the influence of region A in Fig. 11

bl refers to conditions evaluated at the edge of the boundary layer

c refers to conditions at the contact surface

e refers to conditions some distance behind stationary shock wave

L refers to laminar-flow conditions

m refers to values of properties evaluated at mean enthalpy

w/

w	refers to wall conditions
S	refers to quantities measured at room temperature
S_i	refers to shock wave moving into region i
R	refers to flow durations
TH	refers to quantities evaluated from simple shock-tube theory
T	refers to turbulent flow conditions
τ	refers to transition point.

Note that Primes and Bars used with lengths refer to special lengths defined individually.

References

No.	Author(s)	Title, etc.
1	B. D. Henshall	Some notes on the flow durations occurring in hypersonic shock tubes. A.R.C. C.P. 290. August, 1955.
2	R. E. Duff	Shock-tube performance at low initial pressure. Physics of Fluids, Vol.2, No.2. March-April, 1959.
3	A. J. Chabai and E. J. Emrich	Transition from laminar to turbulent flow in the shock tube boundary layer. Bull.Am. Phys. Soc. Sci.II, Vol.3, p.291. 1958.
4	G. F. Anderson	Shock tube testing time. J. Aero/Space Sci., Vol.26, p.184. March, 1959.
5	A. Roshko	On flow duration in low-pressure shock tubes. Physics of Fluids, Vol.3, No.6. November-December, 1960.
6	W. J. Hooker	Testing time and contact-zone phenomena in shock tube flows. Physics of Fluids, Vol.4, No.12. December, 1961.
7	M. Mirels	Laminar boundary layer behind shock advancing into stationary fluid. N.A.C.A. Tech. Note 3401. March, 1955.
8	H. Schlichting	Boundary-layer theory, Chapter 2. McGraw-Hill Book Co. Inc., New York, 1955.
9	L. Bernstein	Notes on some experimental and theoretical results for the boundary layer development aft of a shock in a shock tube. A.R.C. C.P. 625. April, 1961.

10/

References (Continued)

No.	Author(s)	Title, etc.
10	W. A. Martin	An experimental study of the boundary layer behind a moving plane shock. Univ. of Toronto UTIA Rep. No. 47. 1957.
11	D. White	Influence of diaphragm opening times on shock tube flow. J. Fluid Mech. Vol.4, p.585. November, 1958.
12	L. Bernstein	Some measurements of shock-wave attenuation in channels of various cross-sections. A.R.C. R.& M.3321. February, 1961.
13	J. G. Hall	Transition through a contact region. Journ. of Applied Physics, Vol.26, No.6, pp.698-700. June, 1955.
14	J. N. Bradley	Shock waves in chemistry and physics. Chapter 3, p.103. Methuen & Co. Ltd., London. 1962.
15	G. I. Taylor	The instability of liquid surfaces when accelerating in a direction perpendicular to their planes. Proc. Roy. Soc. A, Vol.201, p.192. 1950.
16	L. Bernstein	Tabulated solutions of the equilibrium gas properties behind the incident and reflected normal shock-wave in a shock tube. A.R.C. C.P. 626. April, 1961.
17	I. I. Glass	Shock tubes. Part I. Theory and performance of simple shock tubes. Univ. of Toronto UTIA Review No.12. May, 1958.
18	H. Mirels	Boundary layer behind shock or thin expansion wave moving into stationary fluid. N.A.C.A. Tech. Note 3712. May, 1956.
19	J. P. Appleton and P. J. Musgrove	An investigation of the departure from ideal shock tube performance. Preliminary results. Dept. of Aeronautics and Astronautics. University of Southampton. April, 1963.

APPENDIX I/

APPENDIX I

Some Useful Normal Shock-Wave Relationships

The transformed gas velocity behind the shock wave used in the boundary-layer relationships of Sections 3.2 and 3.3 may be easily obtained by remembering that, due to the velocity transformation used to reduce the shock to rest in the transformed plane,

$$u_{e_0} = W_1 - u_2 ,$$

i.e.

$$\frac{u_{e_0}}{a_1} = M_{S_1} - U_{21} .$$

The value of U_{21} as a function of M_{S_1} may be found in the standard literature[17] on shock tubes and is

$$U_{21} = \frac{1}{M_{S_1}} \left[\frac{M_{S_1}^2 - 1}{\frac{\gamma + 1}{2}} \right] .$$

Therefore

$$\frac{u_{e_0}}{a_1} = \frac{\frac{\gamma-1}{2} M_{S_1}^2 + 1}{\frac{\gamma+1}{2} M_{S_1}} . \qquad \ldots (A.1.1)$$

It may also be shown that

$$\left(\frac{a_2}{a_1} \right)^2 = A_{21}^2 = T_{21} = \frac{4 \left(M_{S_1}^2 - \frac{\gamma-1}{2} \right) \left(\frac{\gamma-1}{2} M_{S_1}^2 + 1 \right)}{M_{S_1}^2 (\gamma+1)^2} \qquad \ldots (A.1.2)$$

Hence since

$$M_{e_0}^2 = \left(\frac{u_{e_0}}{a_1} \right)^2 . A_{12}^2$$

from (A.1.1) and (A.1.2)

$$M_{e_0}^2 = \frac{\frac{\gamma-1}{2} M_{S_1}^2 + 1}{M_{S_1}^2 - \frac{\gamma-1}{2}} \qquad \ldots (A.1.3)$$

The/

The wall velocity in the transformed plane u_w is numerically equal to the shock speed in the physical plane and so

$$u_w = M_{s_1} a_1 . \qquad \ldots (A.1.4)$$

Therefore

$$\frac{u_w}{u_{e_o}} = \frac{\frac{\gamma+1}{2} M_{s_1}^2}{\frac{\gamma-1}{2} M_{s_1}^2 + 1}$$

from equations (A.1.4) and (A.1.1).

APPENDIX II/

APPENDIX II

The Transition Reynolds Number

An attempt has been made by various investigators[3] to correlate transition phenomena encountered in shock-tube problems with data obtained from experiments carried out on flat plates in compressible boundary-layer flow. It has been suggested that the significant length parameter required for the formulation of a transition Reynolds number for the shock-tube problem is the distance travelled by a fluid element before it encounters transition in the boundary layer. It is also assumed that once transition has occurred, the transition point is propagated with the speed of the shock; thus the transition point remains a constant distance behind the moving shock wave.

It is seen in Fig. 16 that considering some fluid element initially at rest in the region ahead of the shock, the element remains at rest throughout the time AB. At time B the element is assumed to be accelerated through the shock wave to the ideal simple theory velocity of u_2. The element then traverses a distance w and encounters transition at τ, the boundary-layer development length at τ being x_τ.

The transition Reynolds number, R_τ, may now be defined as

$$R_\tau = \frac{u_2 w}{\nu_w} \qquad \ldots (A.2.1)$$

where ν_w is the kinematic viscosity at the wall. With this model it is possible to show from the geometry of the (x', t) diagram that

$$R_\tau = \frac{u_{e_o} \cdot x_\tau}{\nu_w} \left(1 - \frac{W_1}{u_{e_o}}\right)^2 \qquad \ldots (A.2.2)$$

where we have also used the mass continuity equation through the shock wave:

$$u_{e_o} \rho_2 = W_1 \rho_1 . \qquad \ldots (A.2.3)$$

It is more convenient to express ν_w in terms of quantities measured ahead of the shock. Consequently if

$$T_w \simeq T_1$$

then

$$\mu_w \simeq \mu_1$$

and remembering that the static pressure is conserved through the boundary layer, it follows that

$$\nu_w = \frac{\mu_1}{\rho_2 T_{21}} .$$

Hence/

Hence:

$$R_T = \frac{W_1 x_T}{\nu_1} T_{21} \left(1 - \frac{W_1}{u_{e_o}}\right)^2 \qquad \ldots (A.2.4)$$

where we have again made use of the expression (A.2.3).

The analysis resulting in the expression (A.2.4) for R_T was first performed by Mirels[18].

It may be preferable to obtain a transition Reynolds number based on the kinematic viscosity of the free stream, i.e.,

$$\bar{R}_T = \frac{u_2 w}{\nu_2} . \qquad \ldots (A.2.5)$$

It then follows, as before, that

$$\bar{R}_T = \frac{u_{e_o} x_T}{\nu_2} \left(1 - \frac{W_1}{u_{e_o}}\right)^2$$

since

$$\nu_2 = \nu_1 . \frac{\mu_2}{\mu_1} . \frac{\rho_1}{\rho_2}$$

$$= \nu_1 . T_{21}^{\omega} \Gamma_{12} .$$

Then

$$\bar{R}_T = \frac{u_{e_o} . x_T}{\nu_1} \Gamma_{21} . T_{12}^{\omega} \left(1 - \frac{W_1}{u_{e_o}}\right)^2 .$$

Hence it follows that

$$\bar{R}_T = R_T T_{12}^{\omega + 1} . \qquad \ldots (A.2.6)$$

We may also write $\bar{R}_T$ as

$$\bar{R}_T = R_{e_o} . \frac{u_2}{u_{e_o}} \frac{w}{\bar{a}}$$

where

$$R_{e_o} = \frac{u_{e_o} \bar{a}}{\nu_2} = M_{S_1} R_1 T_{12}^{\omega} .$$

Consequently

$$\bar{R}_T = M_{S_1} R_1 T_{12}^{\omega} \frac{x_T}{\bar{a}} \left(1 - \frac{W_1}{u_{e_o}}\right)^2 . \qquad \ldots (A.2.7)$$

It will be noted that in the Figs. 6 and 8 where transition is assumed to have occurred, the transition Reynolds numbers shown are evaluated making use of (A.2.4), (A.2.6) and (A.2.7). The boundary-layer development length x_T has been obtained from the analysis of Section 3.2.

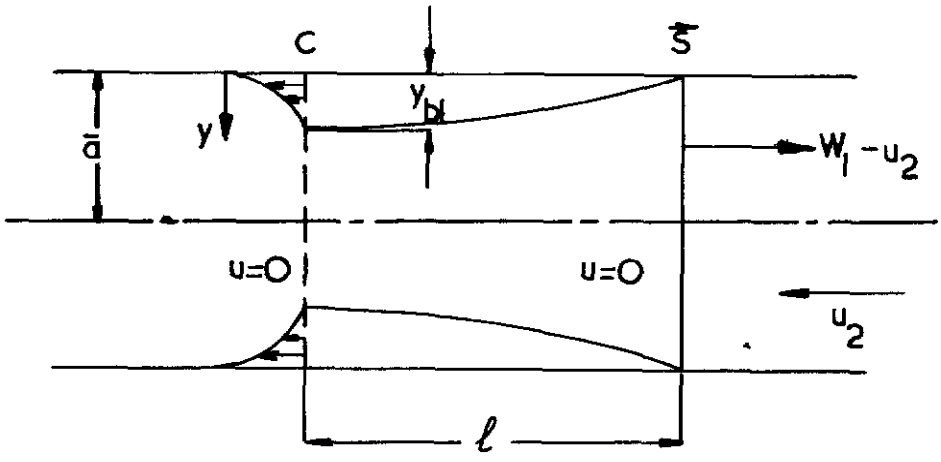

FIG. 1 HOOKER'S MODEL FOR SHOCK-TUBE FLOW RELATIVE TO CONTACT SURFACE

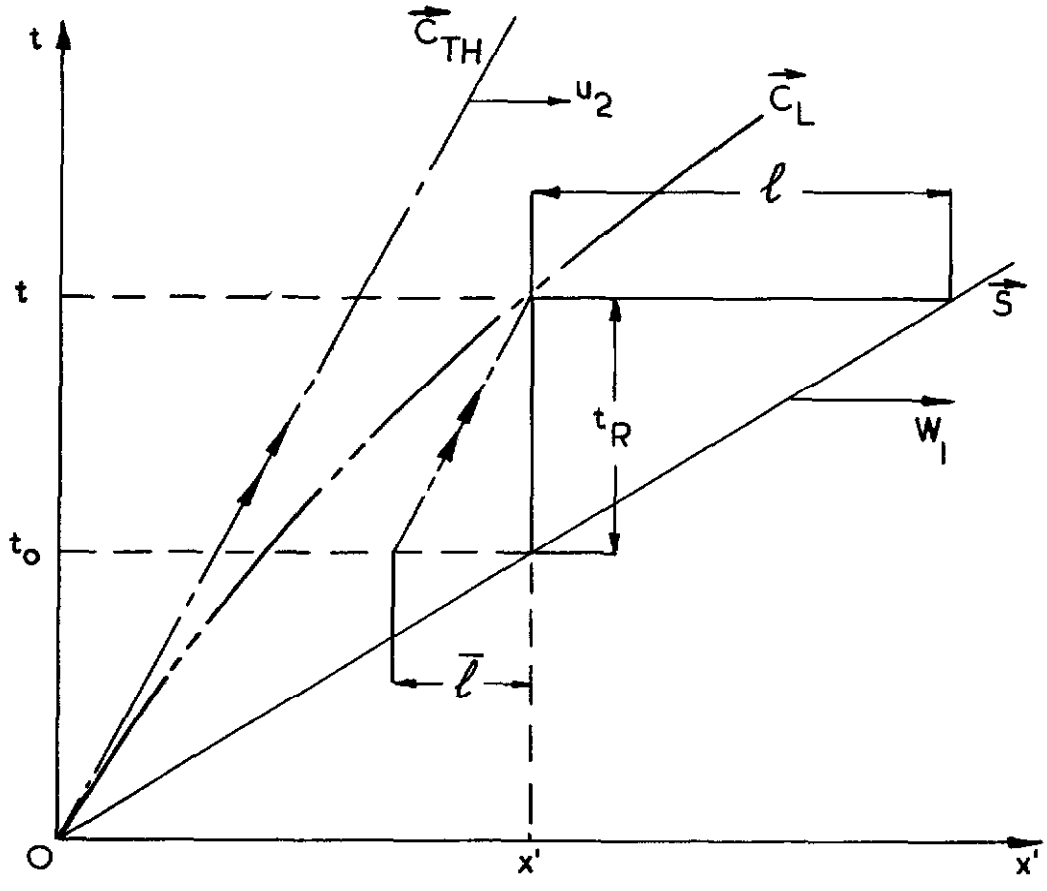

FIG. 2 HOOKER'S INTERPRETATION OF THE (x',t) DIAGRAM

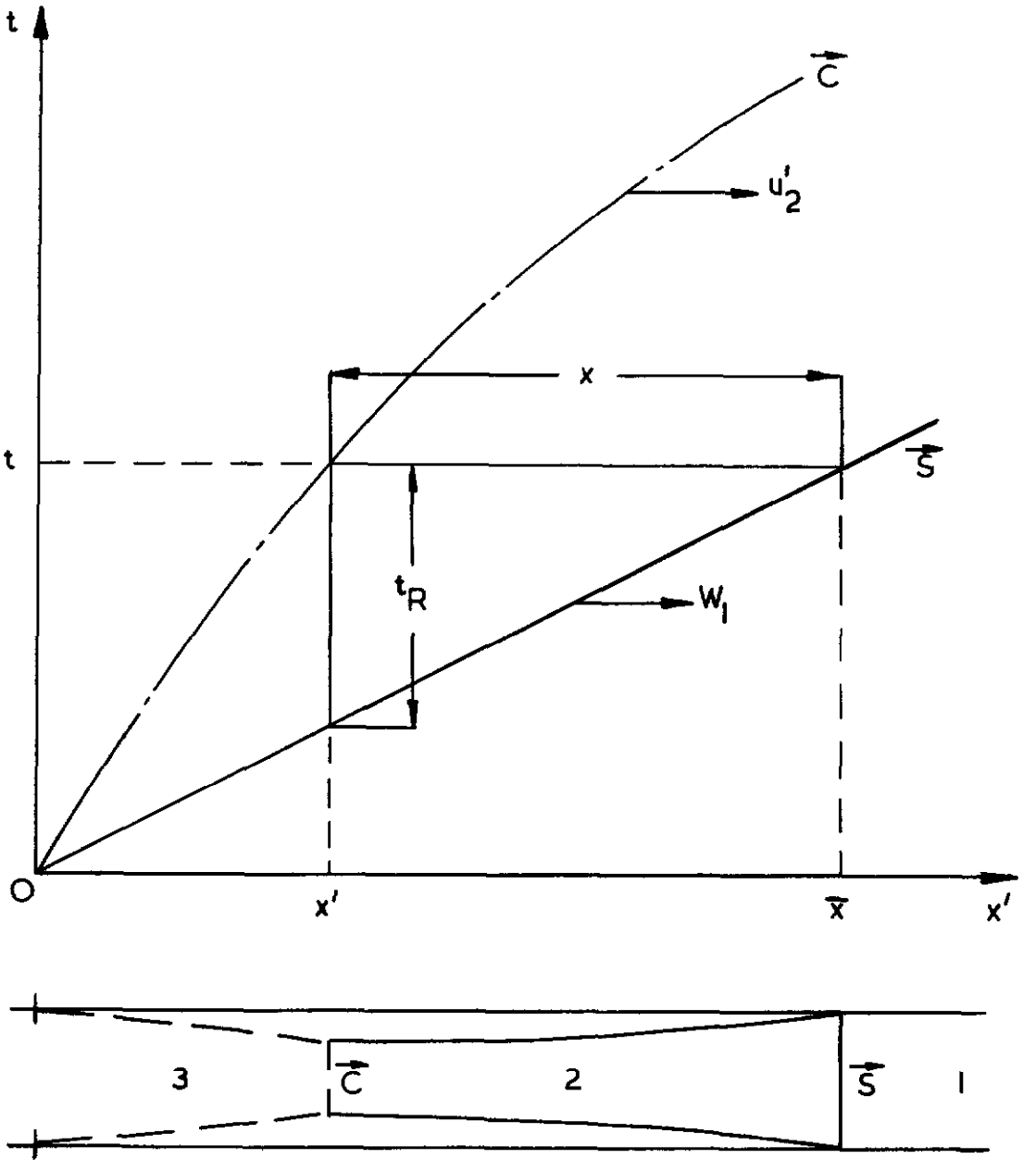

FIG 3. THE (x',t) DIAGRAM FOR THE PRESENT ANALYSIS.

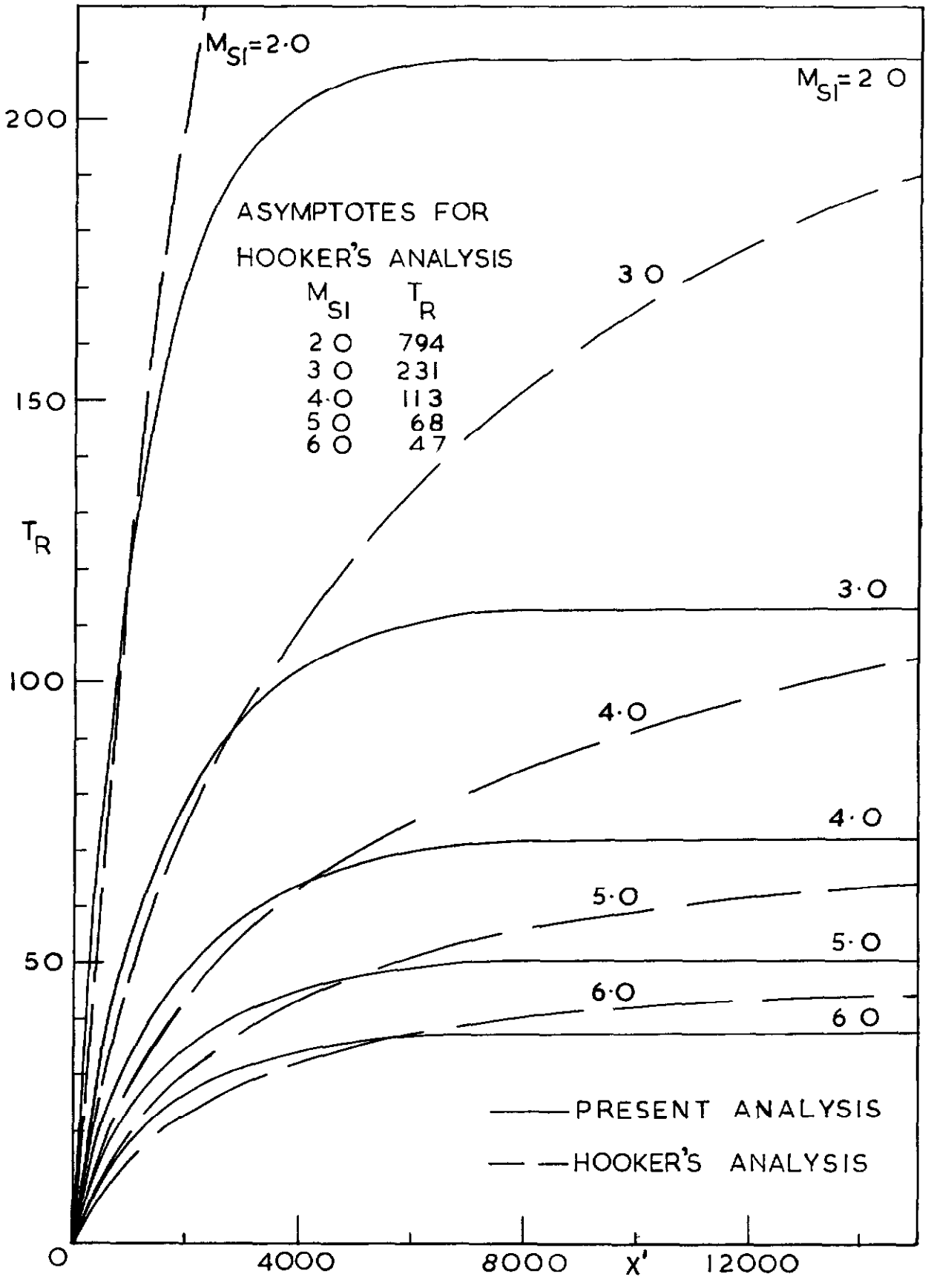

FIG 4a. COMPARISON OF PRESENT ANALYSIS WITH HOOKER'S ANALYSIS, $\gamma = 7/5$.

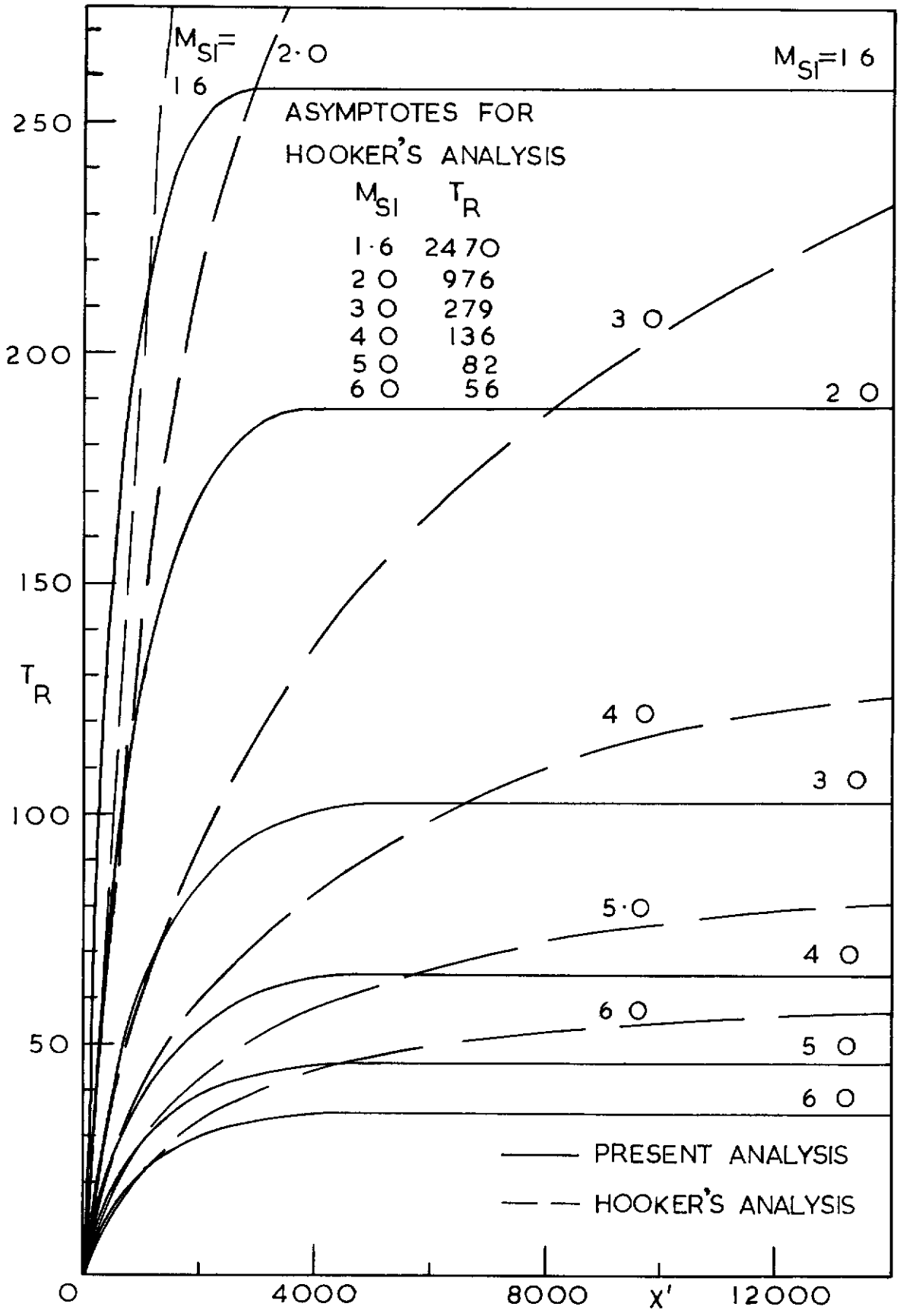

FIG 4b. COMPARISON OF PRESENT ANALYSIS WITH HOOKER'S ANALYSIS, $\gamma = 5/3$

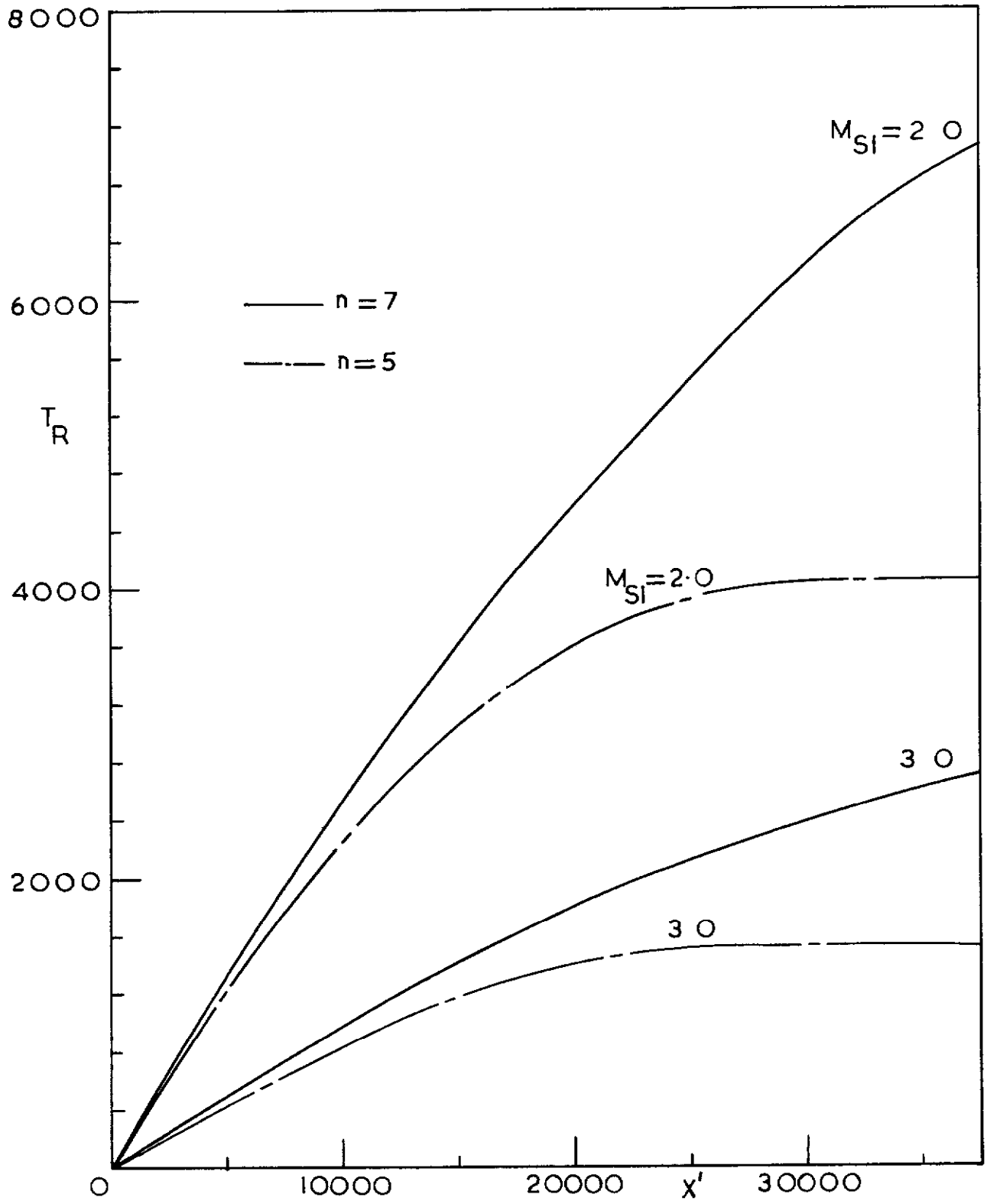

FIG. 5a. TURBULENT-BOUNDARY-LAYER RUNNING-TIME ANALYSIS, $\gamma = 7/5$, $M_{SI} = 2\ 0 \& 3\ 0$

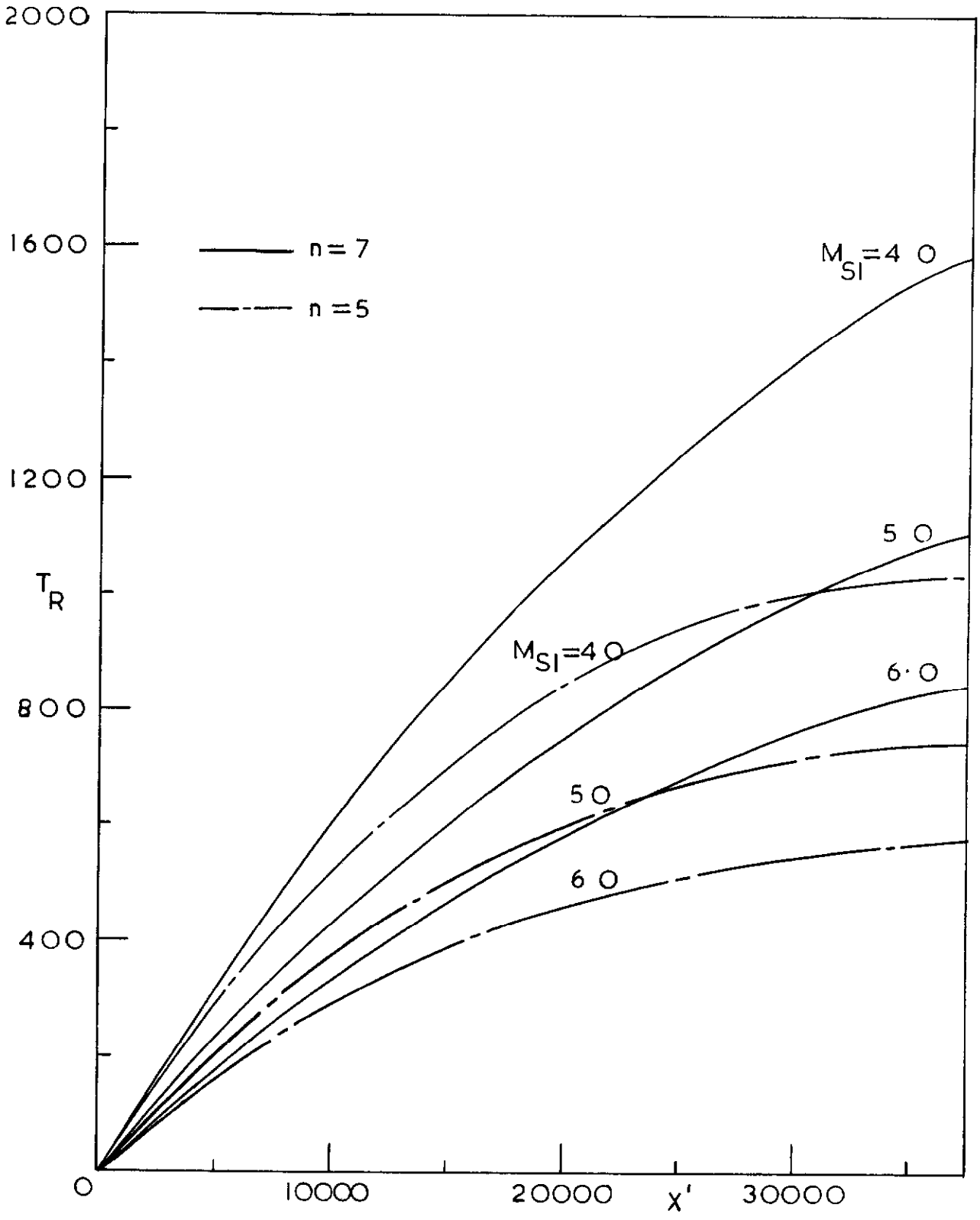

FIG 5b. TURBULENT–BOUNDARY–LAYER RUNNING–TIME ANALYSIS, $\gamma = 7/5$, $M_{SI} = 4\ 0, 5\ 0$ & $6\ 0$

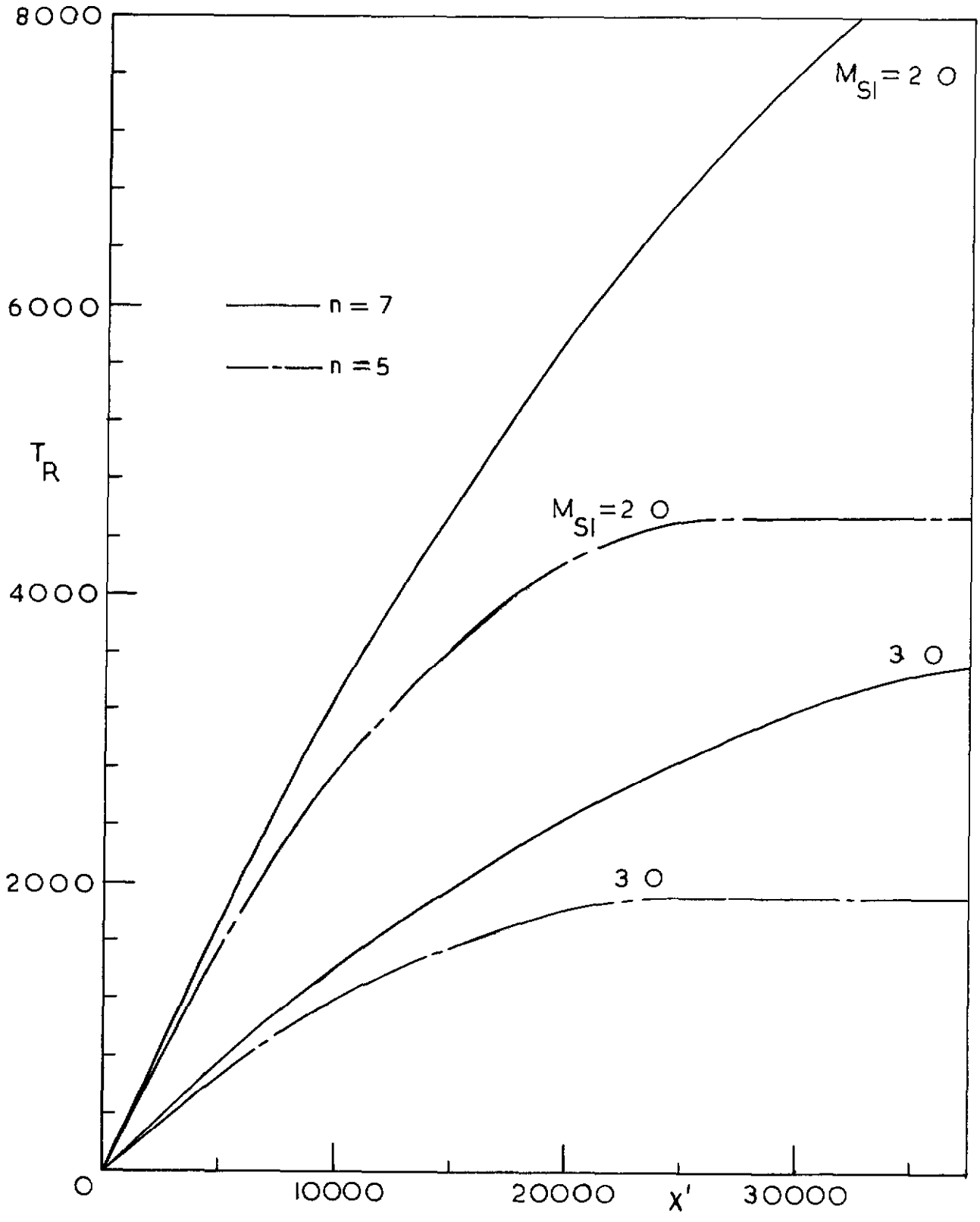

FIG 5c. TURBULENT-BOUNDARY-LAYER RUNNING-TIME ANALYSIS, $\gamma = 5/3$, $M_{SI} = 2\ 0$ & $3\ 0$

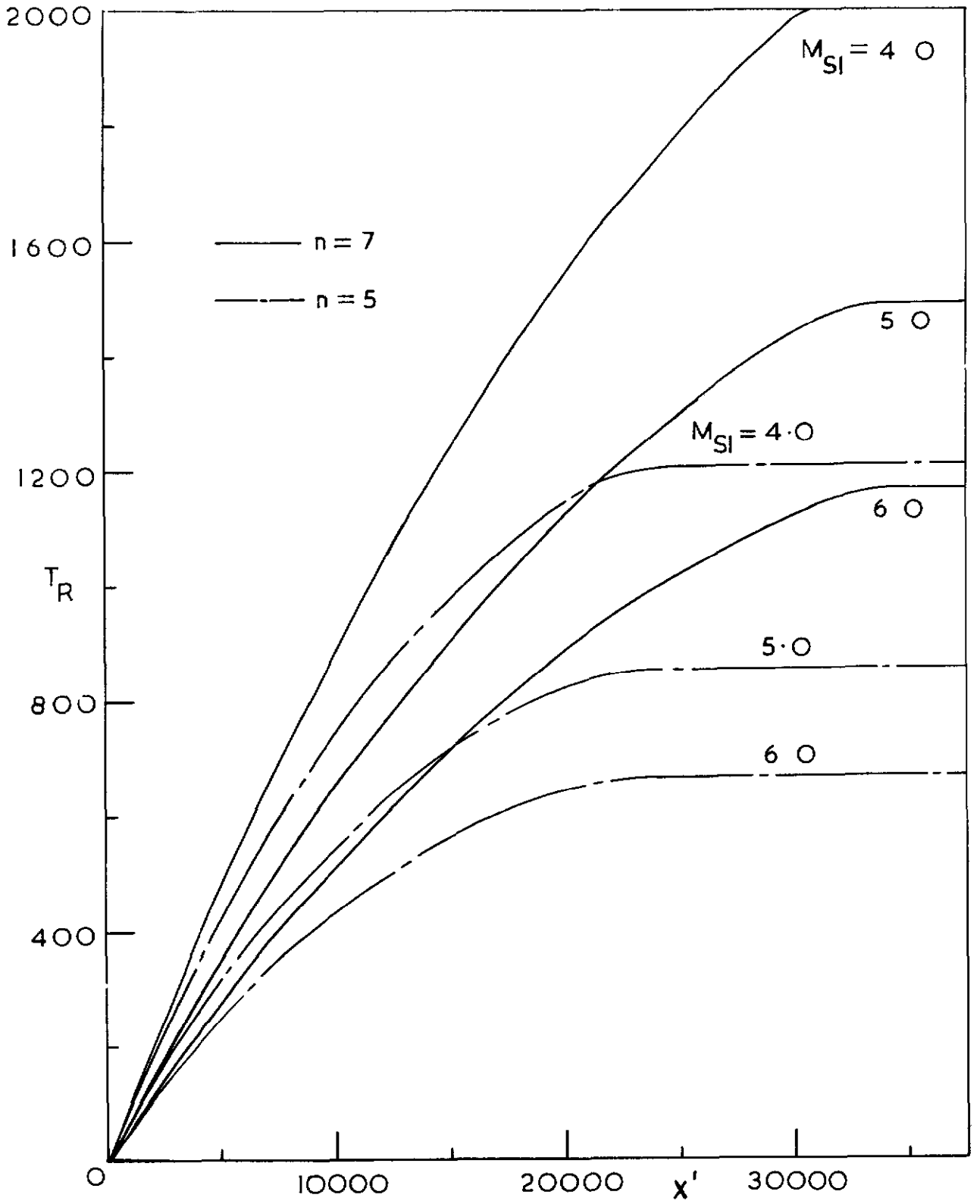

FIG. 5d. TURBULENT-BOUNDARY-LAYER RUNNING-TIME ANALYSIS, $\gamma = 5/3$, M_{SI} = 4 0, 5 0 & 6 0

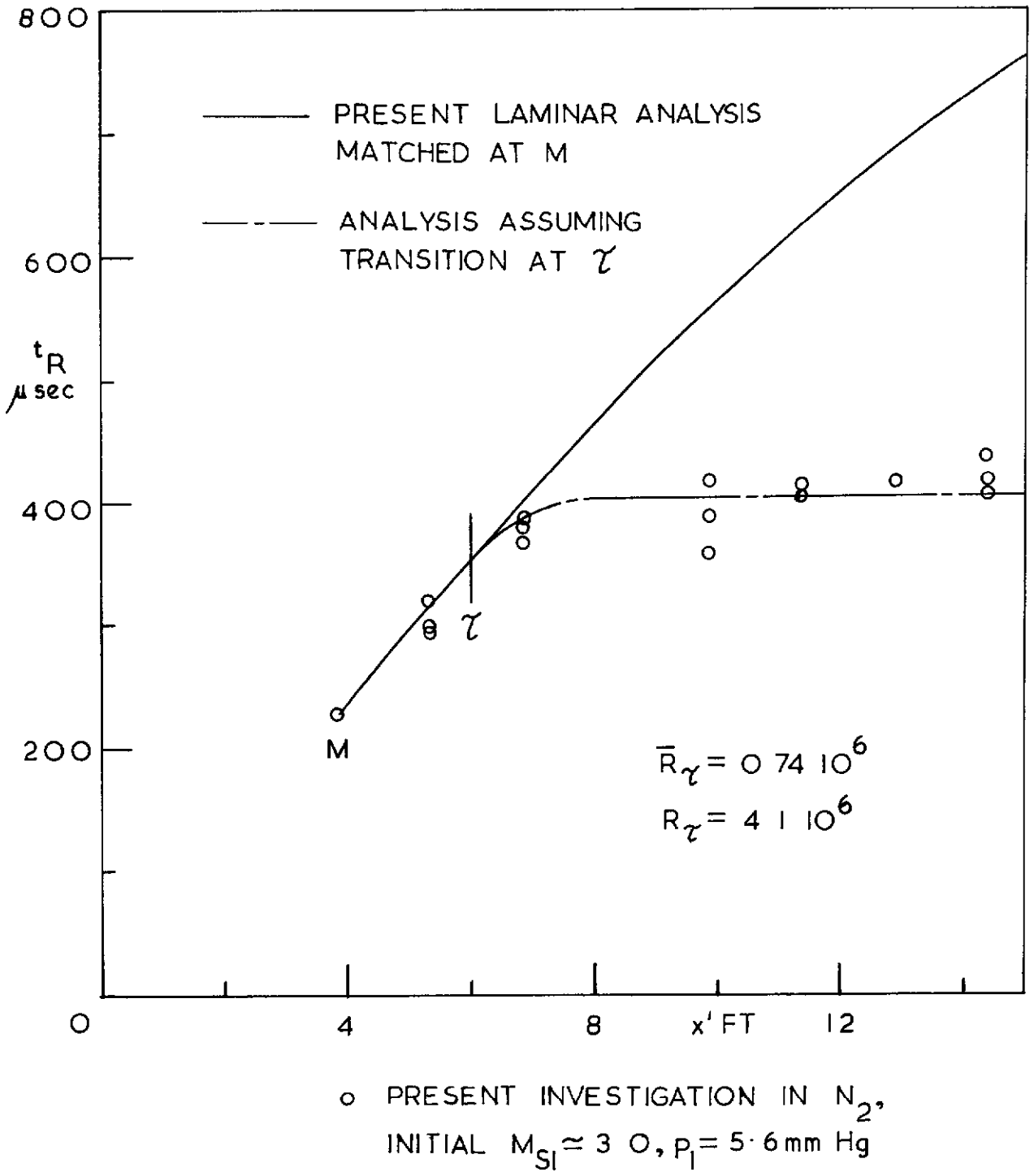

FIG. 6 RUNNING–TIME DISTRIBUTION ALONG CHANNEL

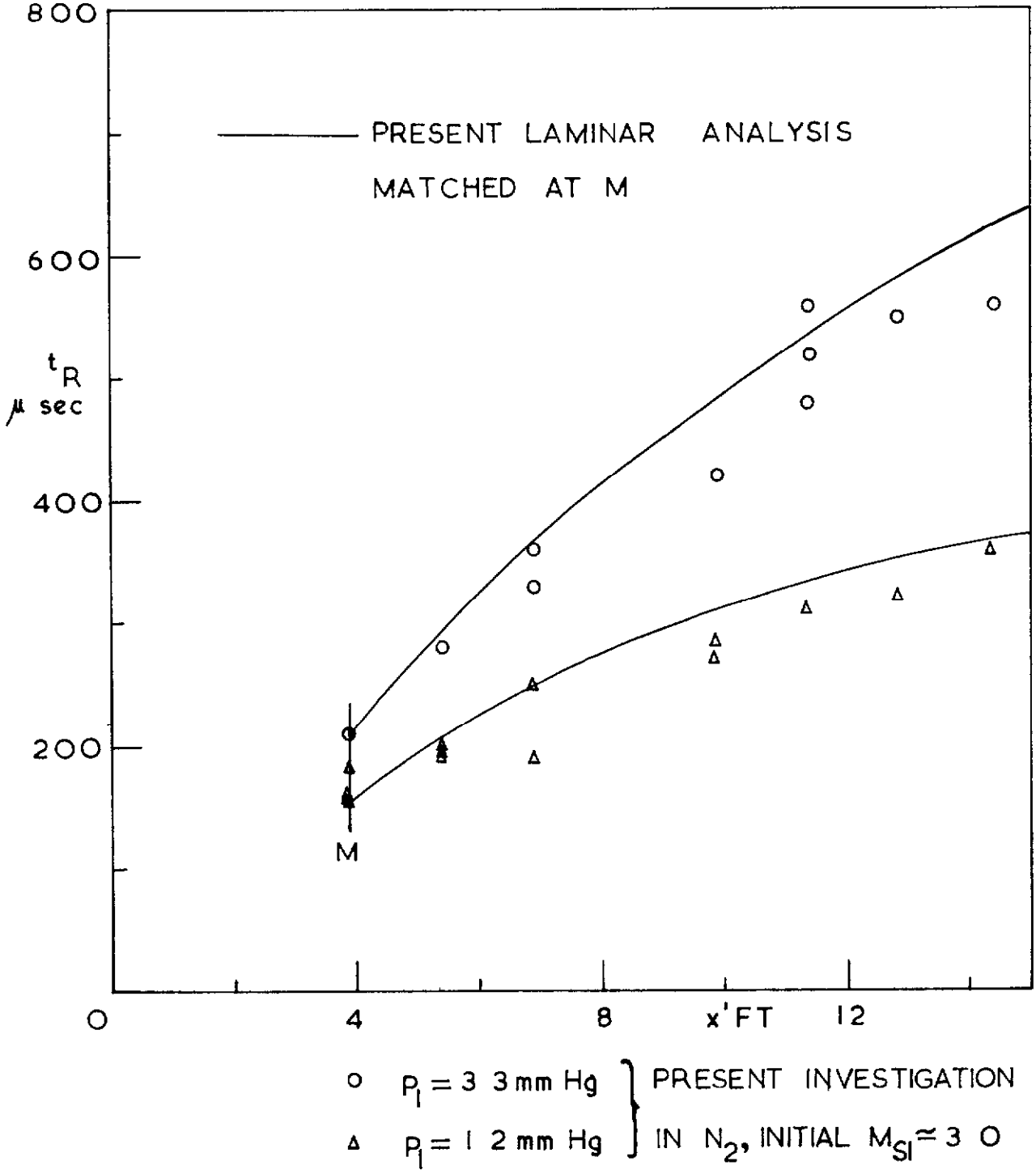

FIG 7. RUNNING-TIME DISTRIBUTION ALONG CHANNEL

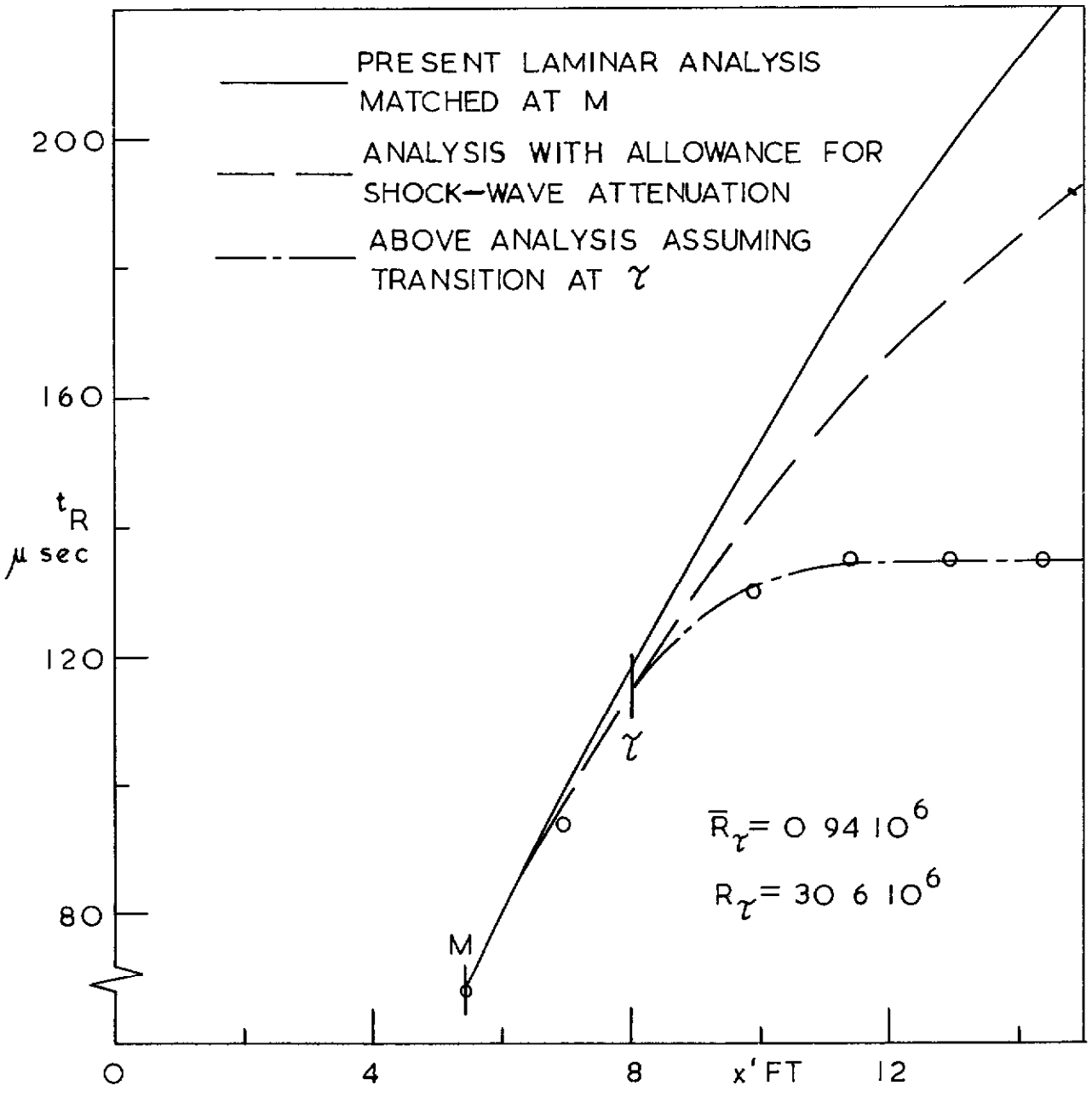

o PRESENT INVESTIGATION IN N_2, INITIAL $M_{SI} \simeq 6\ 0$, $P_1 = 5$mm Hg

FIG. 8. RUNNING-TIME DISTRIBUTION ALONG CHANNEL

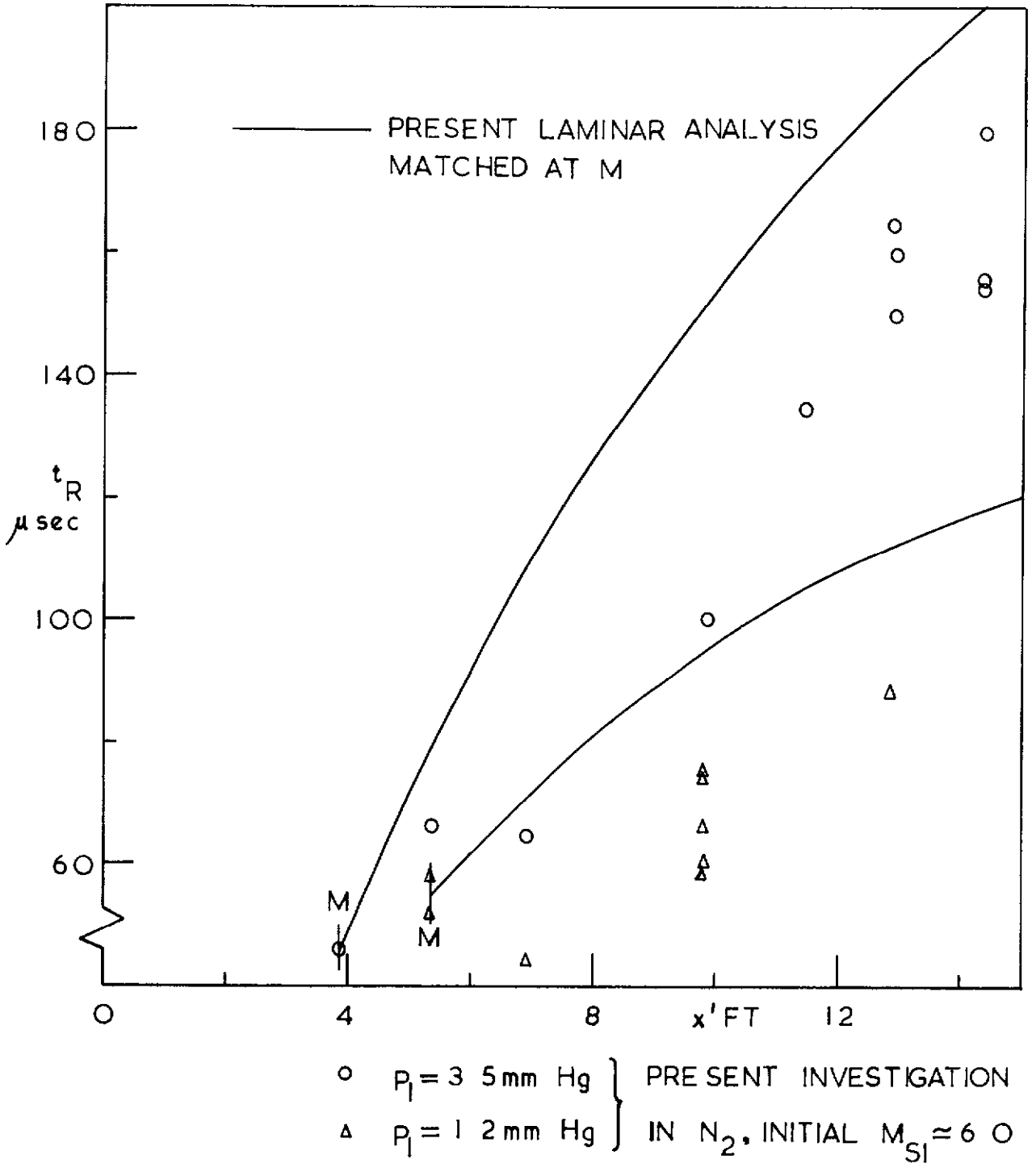

FIG 9. RUNNING-TIME DISTRIBUTION ALONG CHANNEL

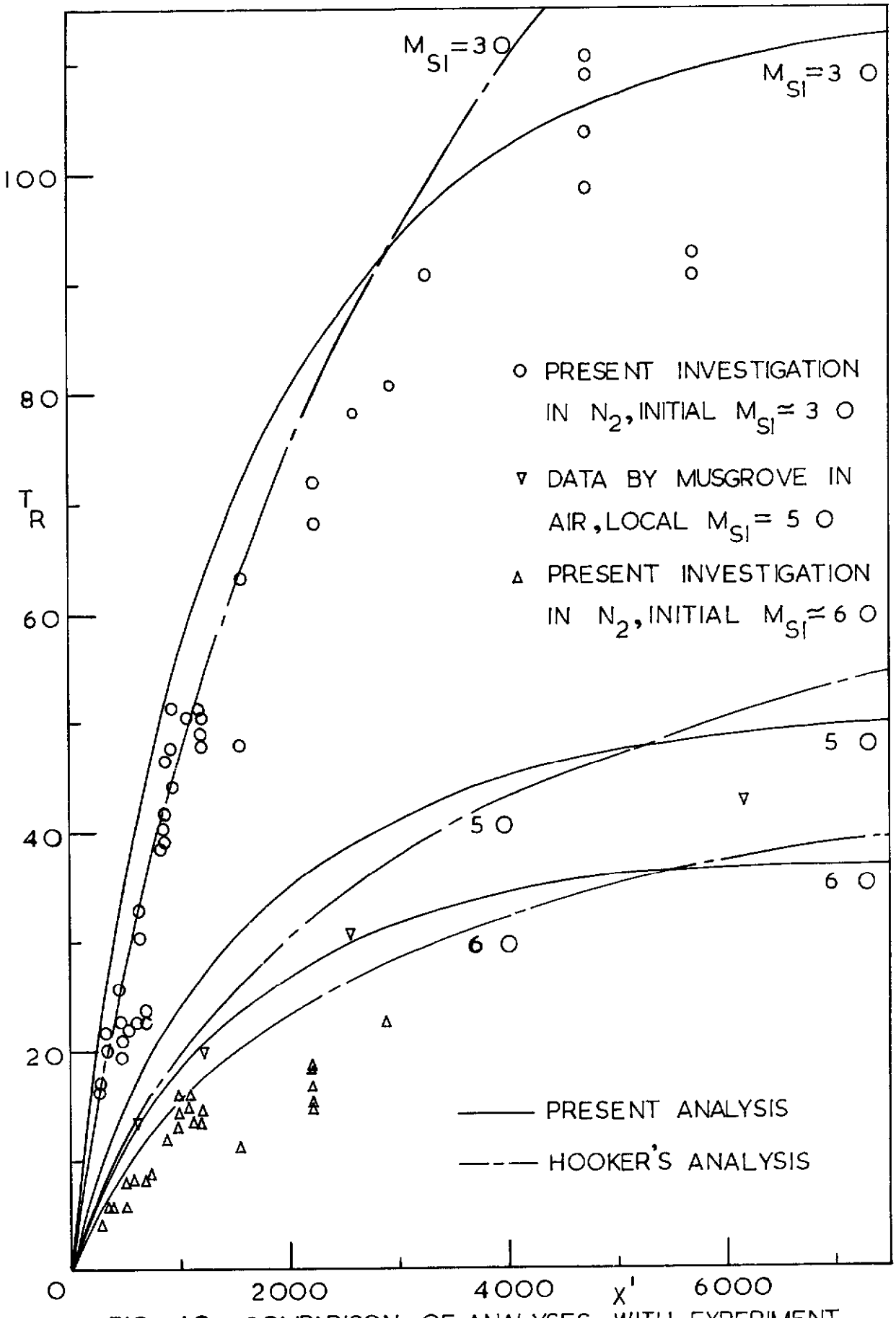

FIG 10a. COMPARISON OF ANALYSES WITH EXPERIMENT, $\gamma = 7/5$

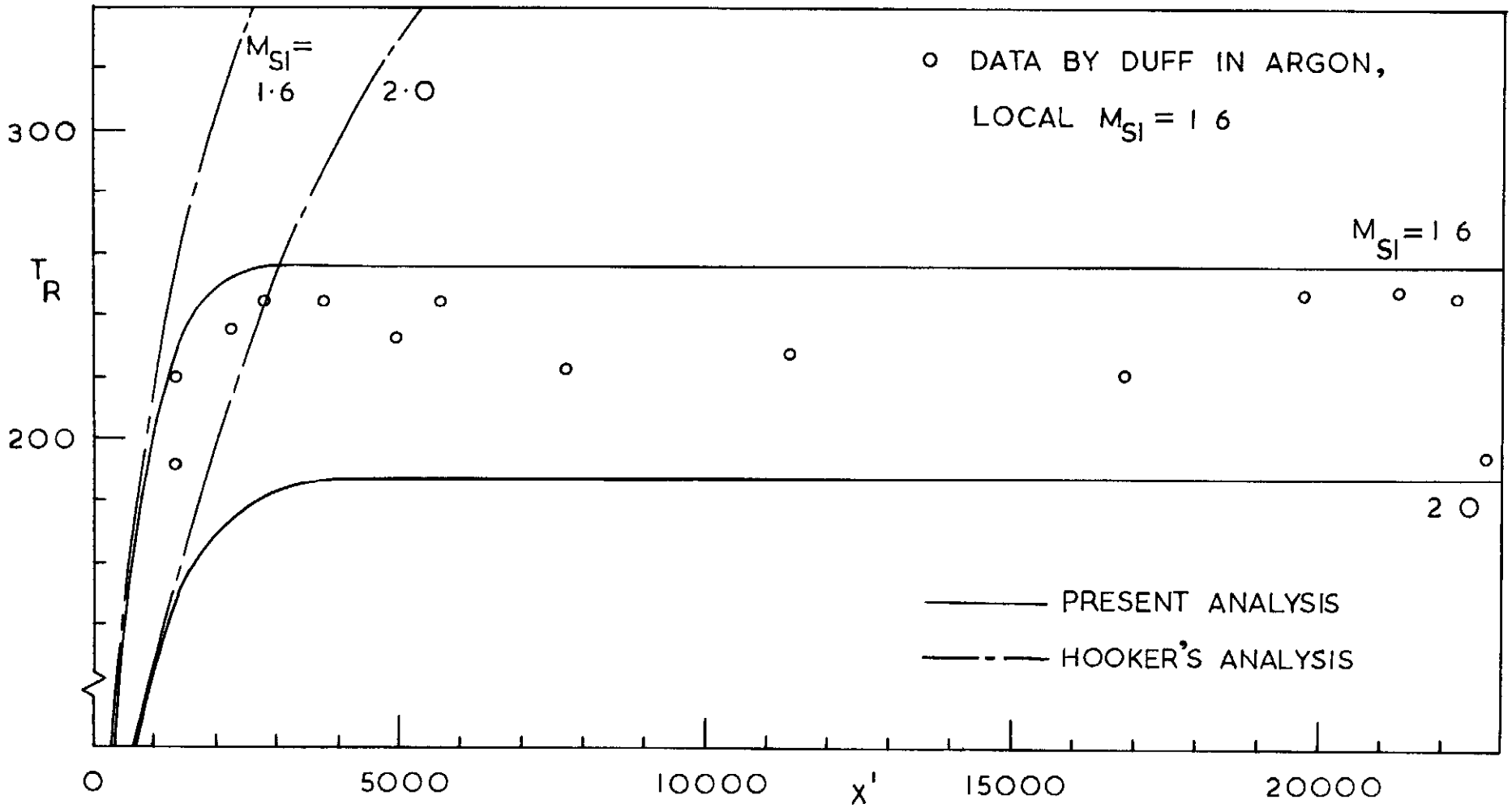

FIG 10b COMPARISON OF ANALYSES WITH EXPERIMENT, $\gamma = 5/3$

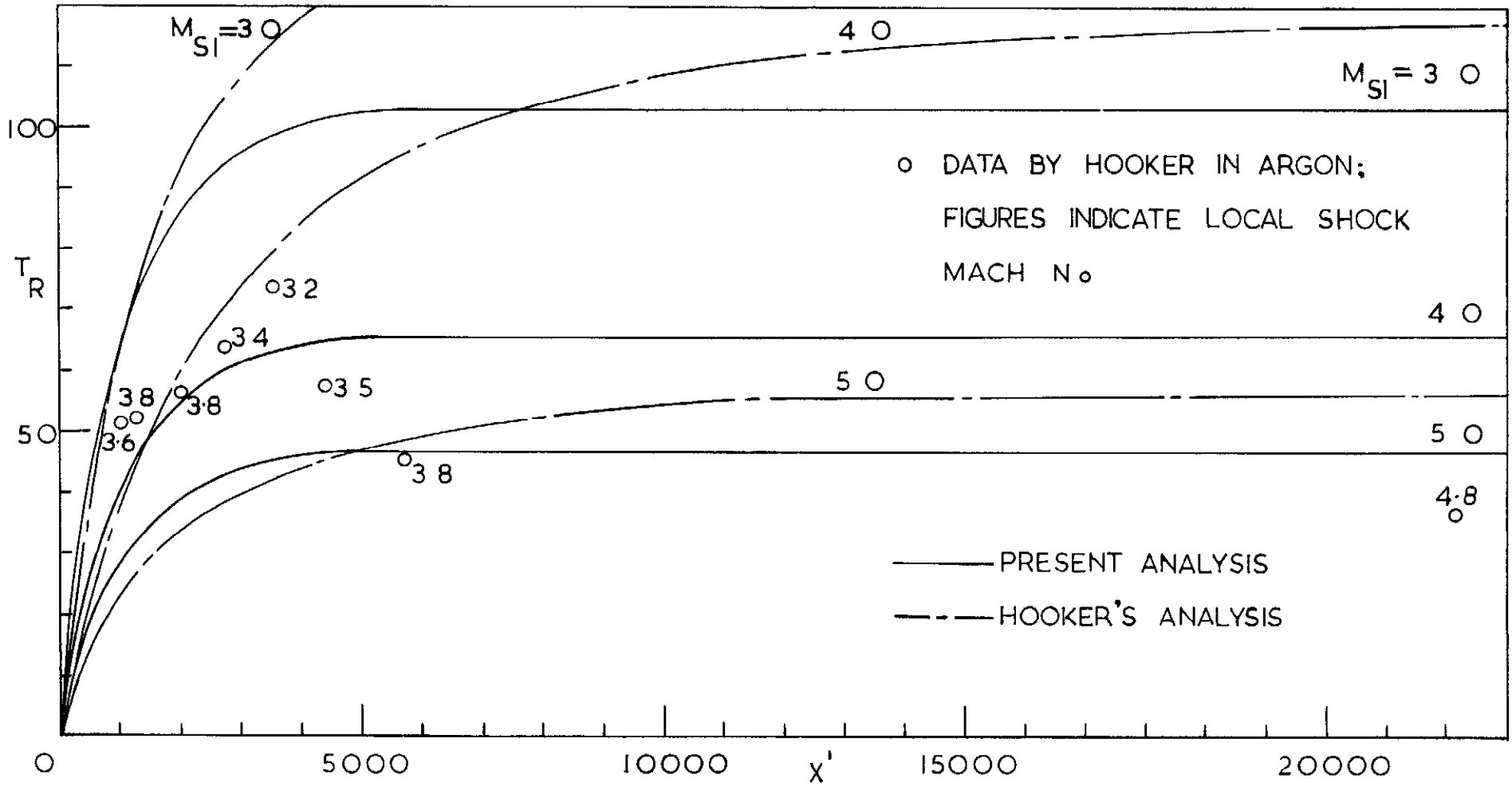

FIG 10c COMPARISON OF ANALYSES WITH EXPERIMENT, $\gamma = 5/3$

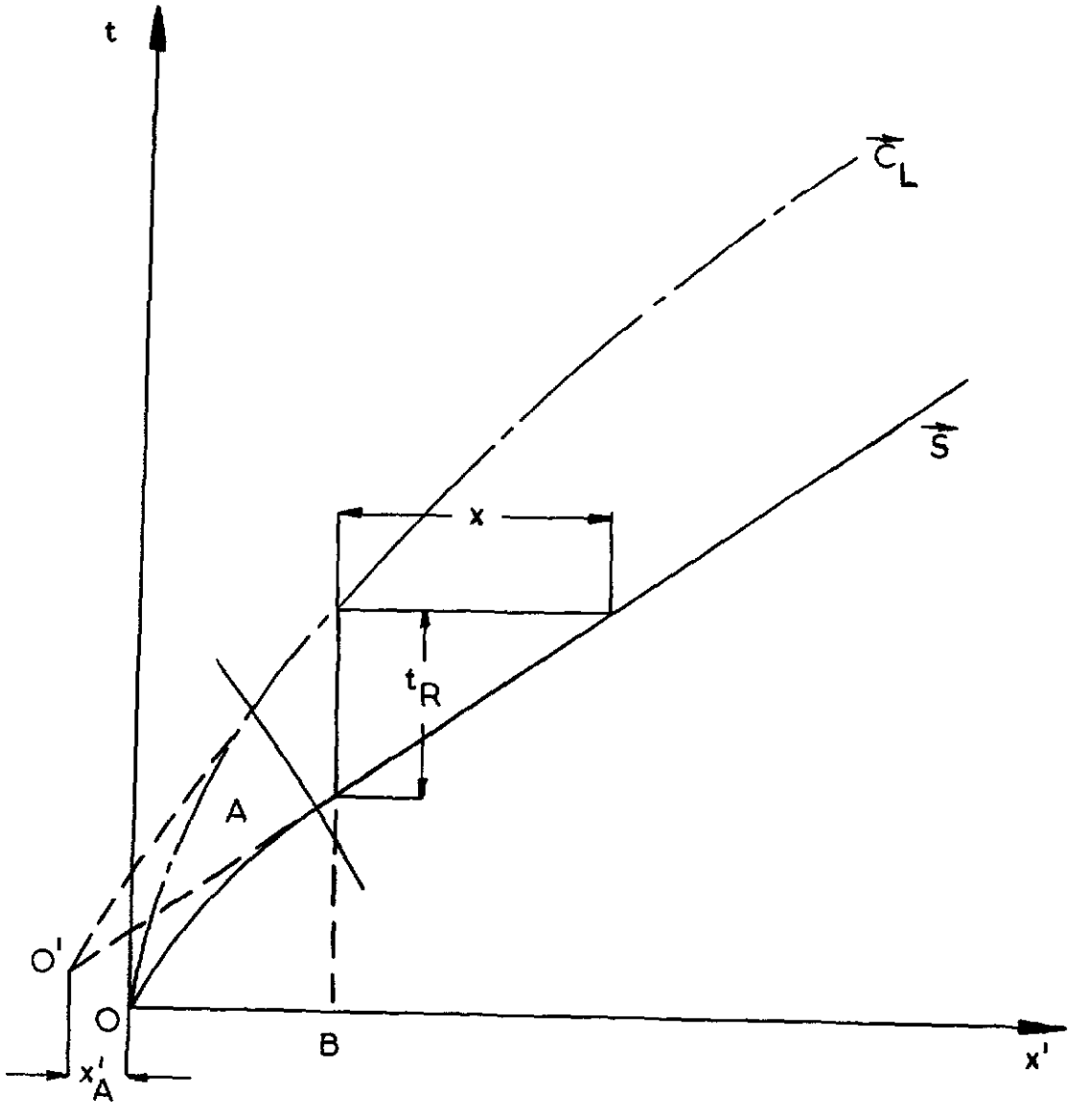

FIG 11. THE (x',t) DIAGRAM SHOWING EFFECT OF FINITE BURSTING TIME OF DIAPHRAGM

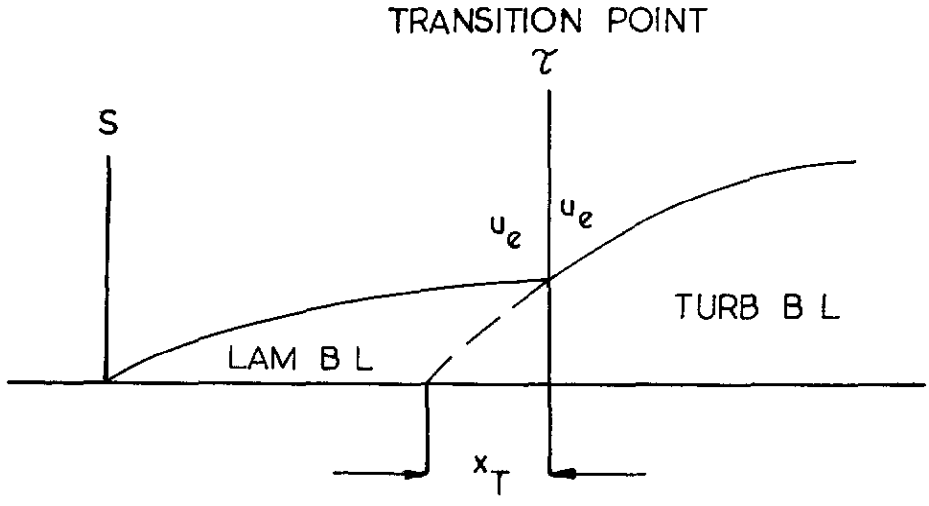

(a)

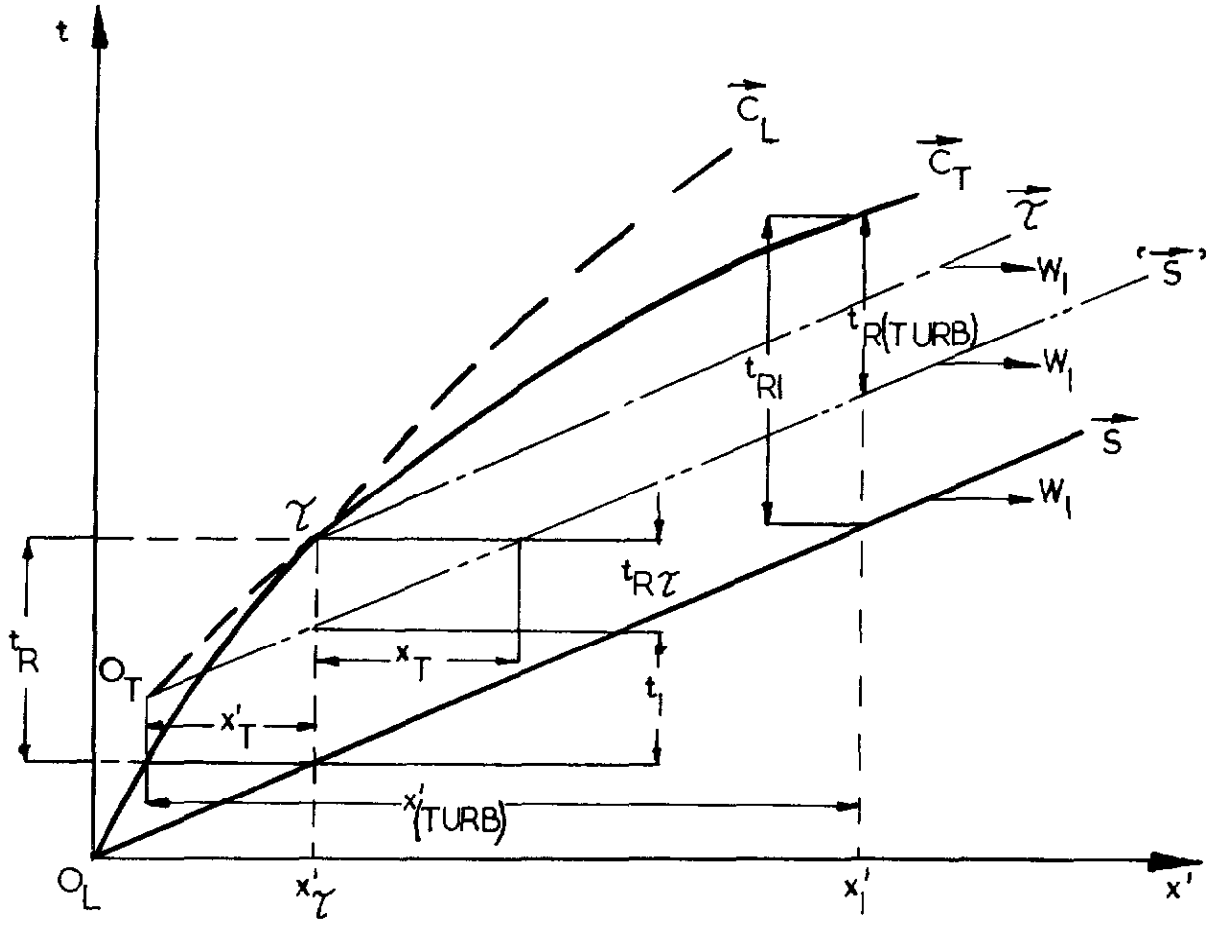

(b)

FIG 12. THE EFFECT OF TURBULENT TRANSITION ON RUNNING TIME

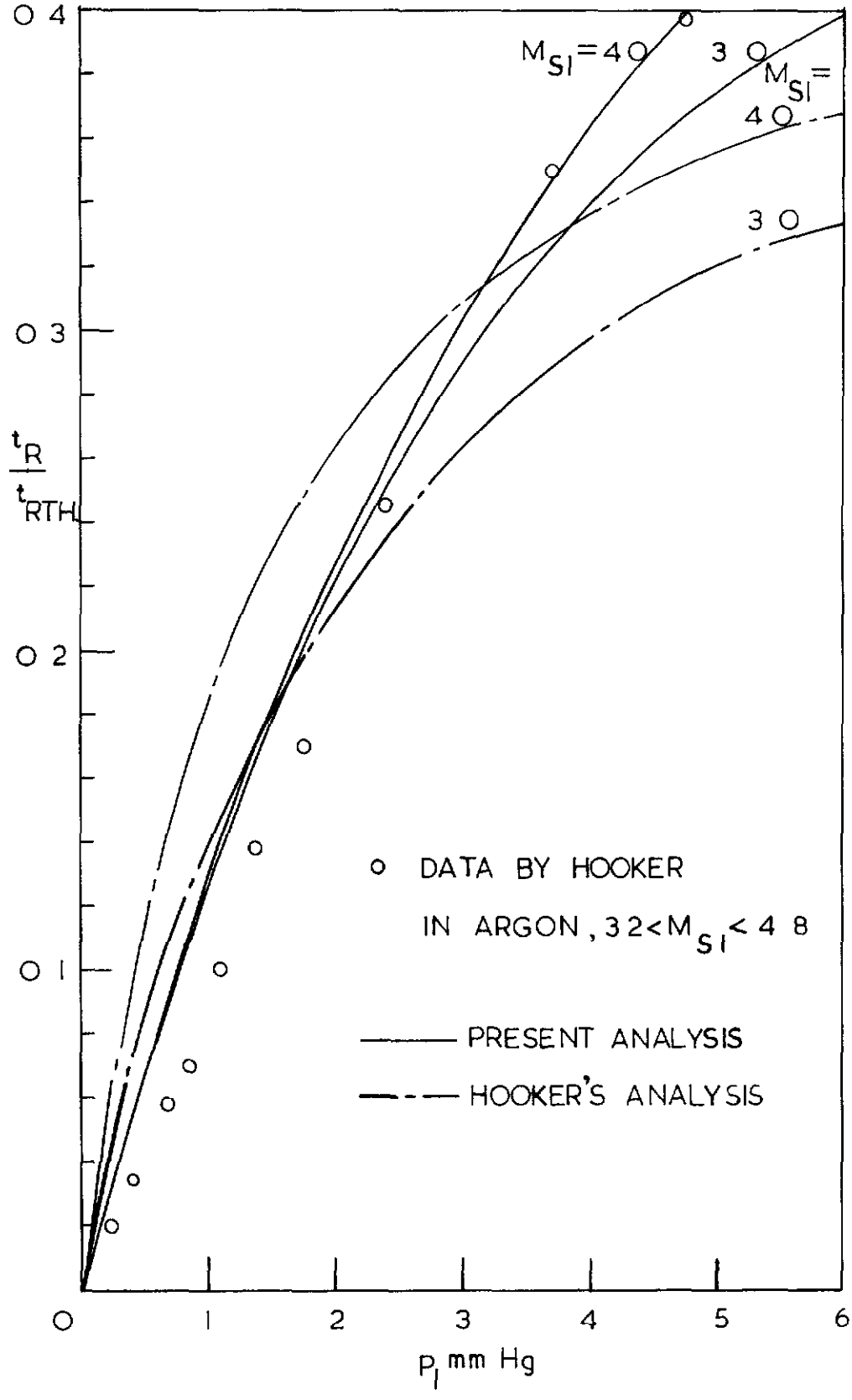

FIG 13a COMPARISON OF ANALYSES WITH EXPERIMENT, $\gamma = 5/3$

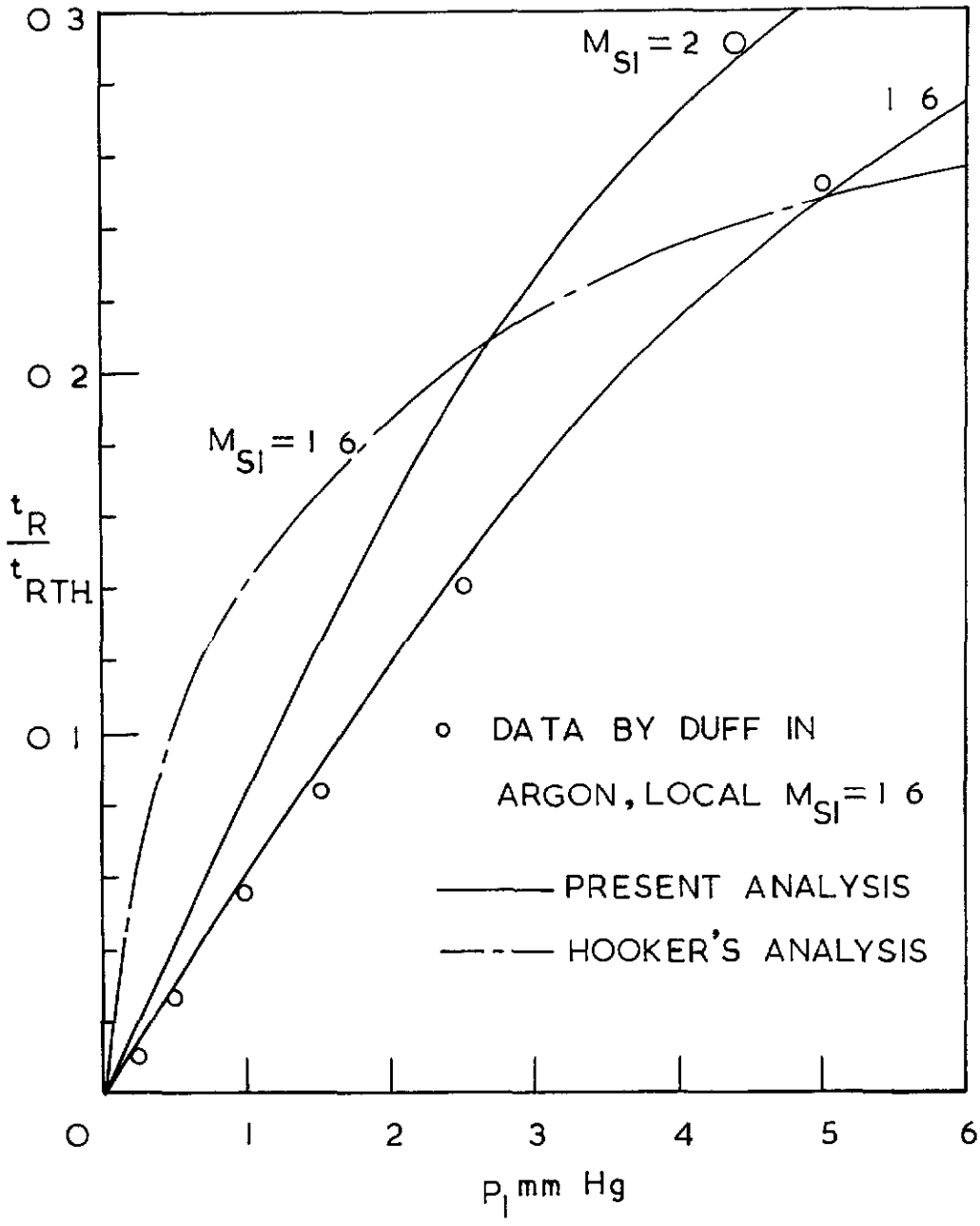

FIG 13b COMPARISON OF ANALYSES WITH EXPERIMENT, $\gamma = 5/3$

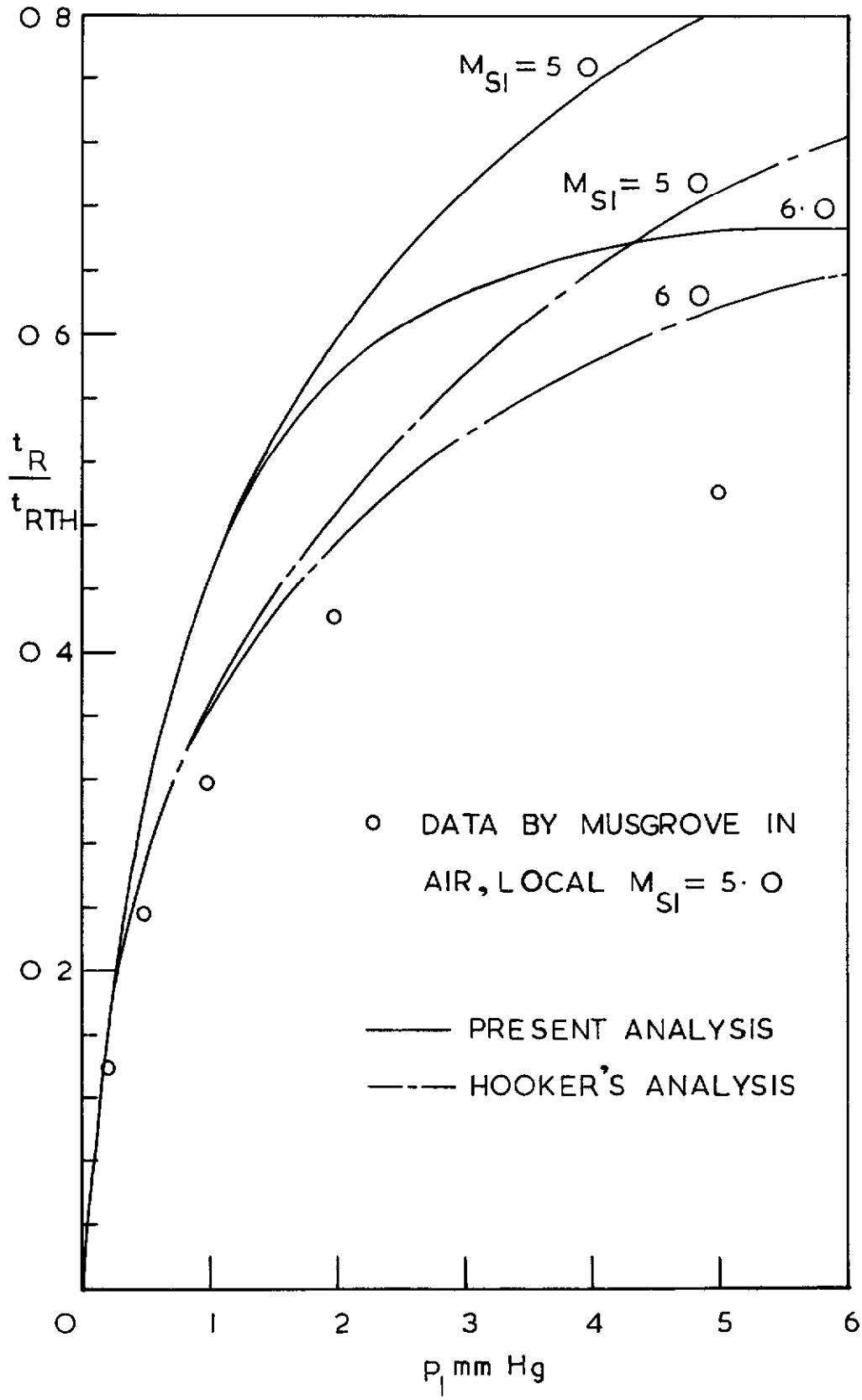

FIG 13c COMPARISON OF ANALYSES WITH EXPERIMENT, $\gamma = 7/5$

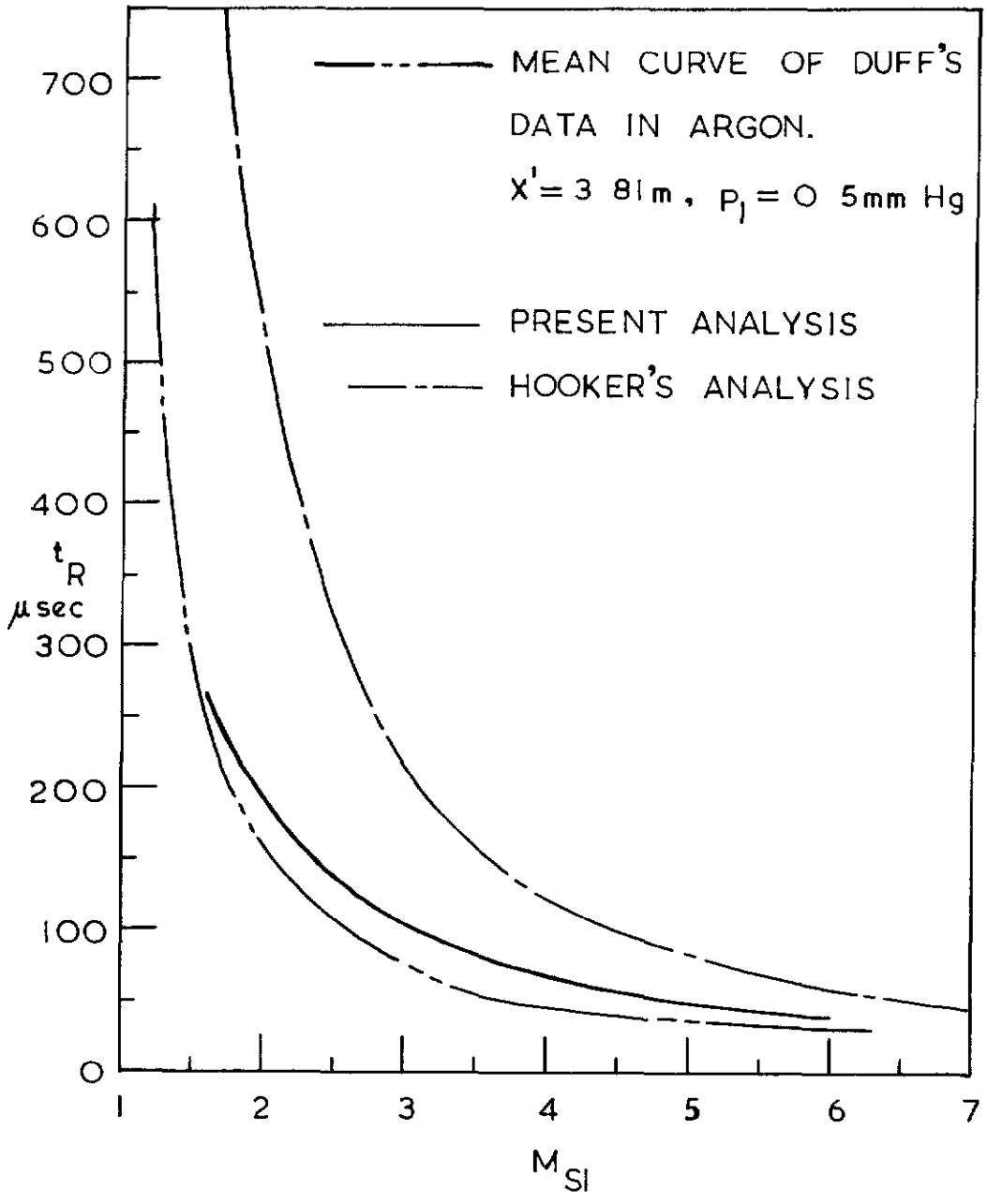

FIG. 14a COMPARISON OF ANALYSES WITH EXPERIMENT, $\gamma = 5/3$: RUNNING TIME AGAINST SHOCK MACH NUMBER.

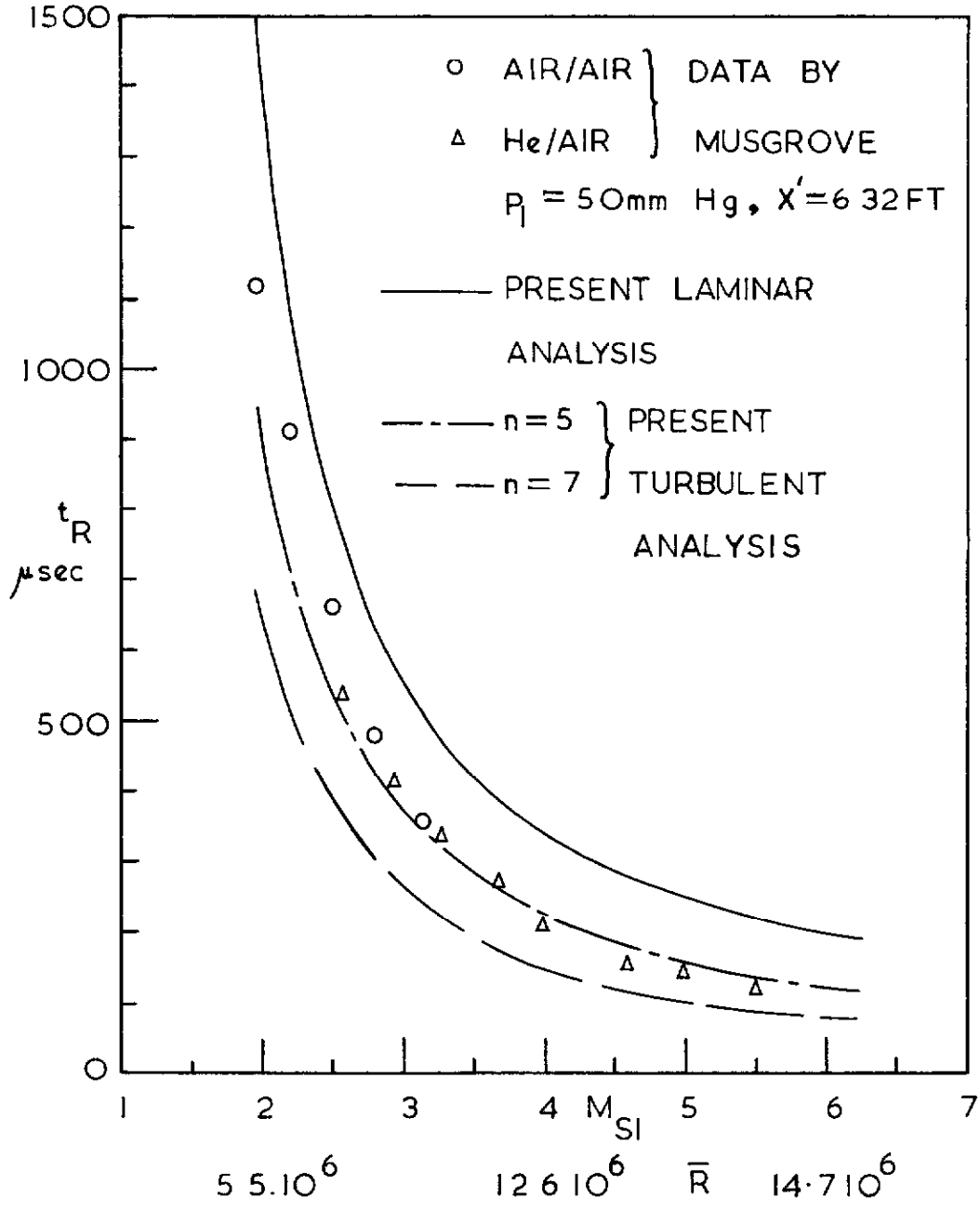

FIG 14b COMPARISON OF ANALYSES WITH EXPERIMENT, $\gamma = 7/5$ RUNNING TIME AGAINST SHOCK MACH NUMBER

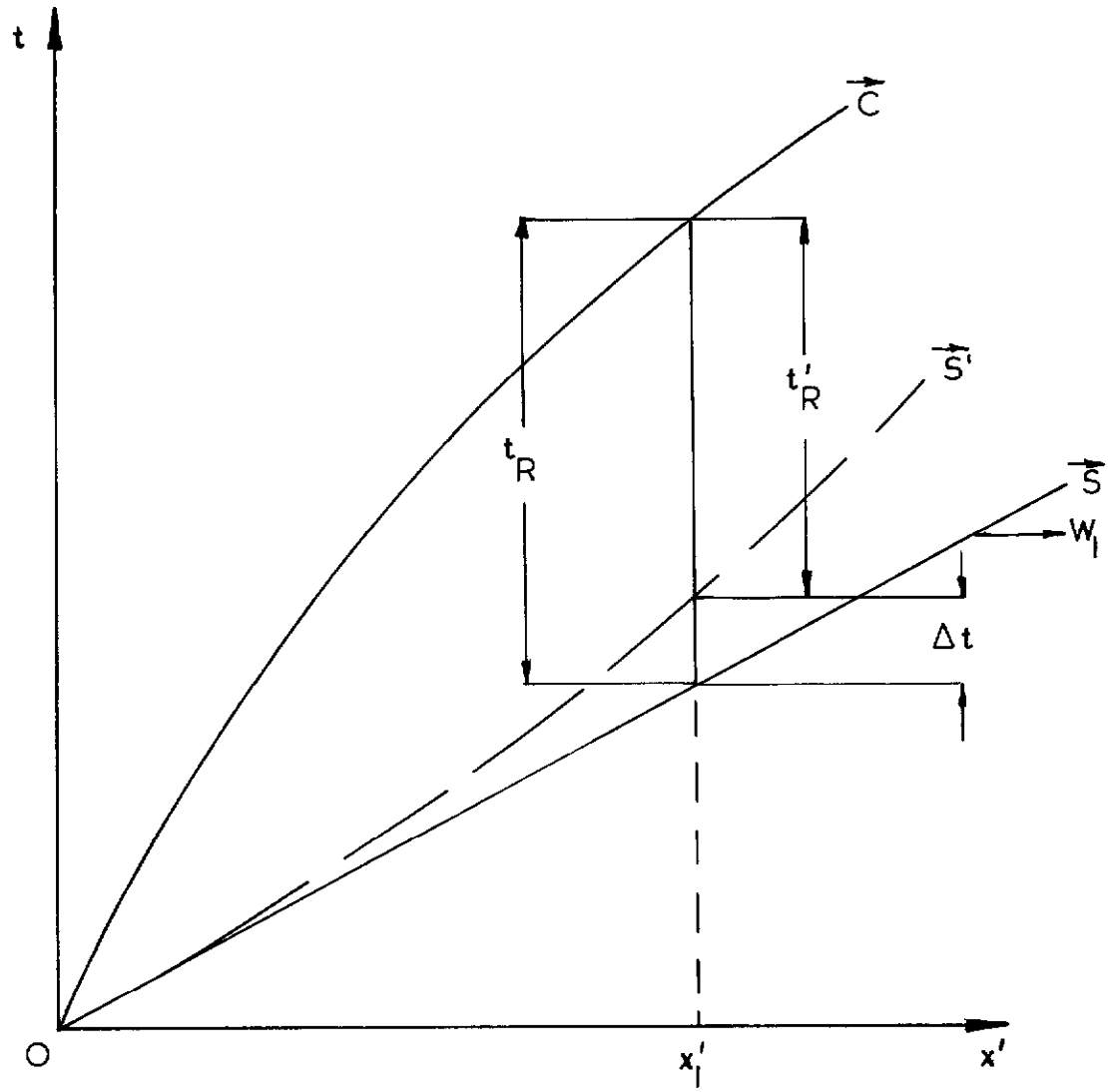

Actual running time at x'_1, t'_R given by

$$t'_R = t_R - \Delta t$$

where t_R is given by the present analysis

FIG 15. A CORRECTION TO THE PRESENT ANALYSIS FOR SHOCK-WAVE ATTENUATION

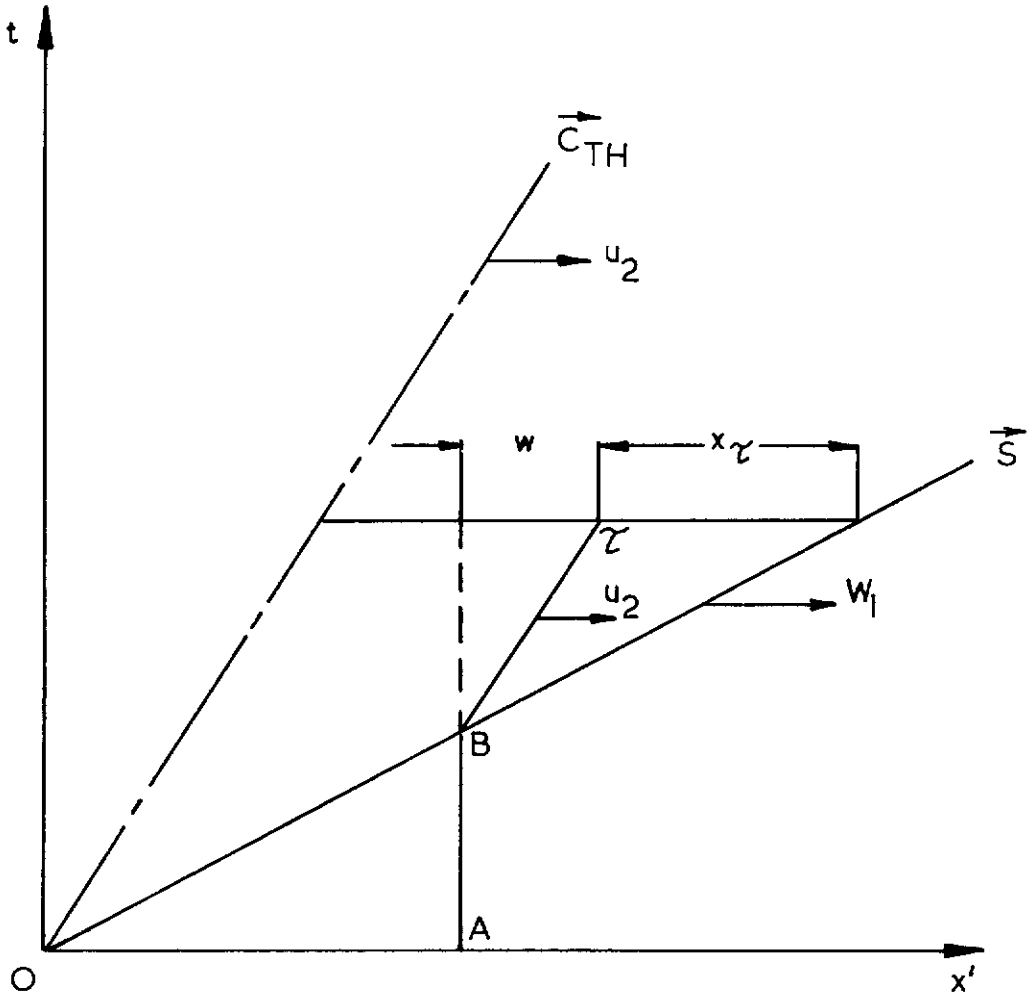

FIG 16. THE SUGGESTED MODEL FOR THE FORMULATION OF A TRANSITION REYNOLDS NUMBER

A.R.C. C.P. No. 722
July, 1963
J. A. D. Ackroyd

A STUDY ON THE RUNNING TIMES IN SHOCK TUBES

A theoretical analysis is presented for the shock-tube running-time problem which differs in certain essentials from previous theories and in particular it does not involve the assumption that the boundary-layer thickness is always small in relation to the shock-tube radius. Experimental results are presented covering a range of initial channel pressures and shock Mach numbers and these, in combination with the results of other workers, are compared with the predictions of the present theory and also those of earlier theories. The present theory is shown to lead to the best agreement, particularly at low initial channel pressures and low shock Mach numbers.

A.R.C. C.P. No. 722
July, 1963
J. A. D. Ackroyd

A STUDY ON THE RUNNING TIMES IN SHOCK TUBES

A theoretical analysis is presented for the shock-tube running-time problem which differs in certain essentials from previous theories and in particular it does not involve the assumption that the boundary-layer thickness is always small in relation to the shock-tube radius. Experimental results are presented covering a range of initial channel pressures and shock Mach numbers and these, in combination with the results of other workers, are compared with the predictions of the present theory and also those of earlier theories. The present theory is shown to lead to the best agreement, particularly at low initial channel pressures and low shock Mach numbers.

A.R.C. C.P. No. 722
July, 1963
J. A. D. Ackroyd

A STUDY ON THE RUNNING TIMES IN SHOCK TUBES

A theoretical analysis is presented for the shock-tube running-time problem which differs in certain essentials from previous theories and in particular it does not involve the assumption that the boundary-layer thickness is always small in relation to the shock-tube radius. Experimental results are presented covering a range of initial channel pressures and shock Mach numbers and these, in combination with the results of other workers, are compared with the predictions of the present theory and also those of earlier theories. The present theory is shown to lead to the best agreement, particularly at low initial channel pressures and low shock Mach numbers.

DETACHABLE ABSTRACT CARDS